Neurobiology of Disease

Anandamide–CB_1 Receptor Signaling Contributes to Postnatal Ethanol-Induced Neonatal Neurodegeneration, Adult Synaptic, and Memory Deficits

Shivakumar Subbanna,[1] Madhu Shivakumar,[1] Delphine Psychoyos,[2] Shan Xie,[1] and Balapal S. Basavarajappa[1,3,4]

[1]Division of Analytical Psychopharmacology, Nathan Kline Institute for Psychiatric Research, Orangeburg, New York 10962, [2]Institute of Biosciences and Technology, Texas A & M University Health Science Center, Houston, Texas 77030, and [3]New York State Psychiatric Institute and [4]Department of Psychiatry, College of Physicians and Surgeons, Columbia University, New York, New York 10032

The transient exposure of immature rodents to ethanol during postnatal day 7 (P7), which is comparable with the third trimester in human pregnancy, induces synaptic dysfunctions. However, the molecular mechanisms underlying these dysfunctions are still poorly understood. Although the endocannabinoid system has been shown to be an important modulator of ethanol sensitivity in adult mice, its potential role in synaptic dysfunctions in mice exposed to ethanol during early brain development is not examined. In this study, we investigated the potential role of endocannabinoids and the cannabinoid receptor type 1 (CB_1R) in neonatal neurodegeneration and adult synaptic dysfunctions in mice exposed to ethanol at P7. Ethanol treatment at P7, which induces neurodegeneration, increased anandamide (AEA) but not 2-arachidonylglycerol biosynthesis and CB_1R protein expression in the hippocampus and cortex, two brain areas that are important for memory formation and storage, respectively. N-Arachidonoyl phosphatidylethanolamine–phospholipase D (NAPE–PLD), glycerophosphodiesterase (GDE1), and CB_1R protein expression were enhanced by transcriptional activation of the genes encoding NAPE–PLD, GDE1, and CB_1R proteins, respectively. In addition, ethanol inhibited ERK1/2 and AKT phosphorylation. The blockade of CB_1Rs before ethanol treatment at P7 relieved ERK1/2 but not AKT phosphorylation and prevented neurodegeneration. CB_1R knock-out mice exhibited no ethanol-induced neurodegeneration and inhibition of ERK1/2 phosphorylation. The protective effects of CB_1R blockade through pharmacological or genetic deletion resulted in normal adult synaptic plasticity and novel object recognition memory in mice exposed to ethanol at P7. The AEA/CB_1R/pERK1/2 signaling pathway may be directly responsible for the synaptic and memory deficits associated with fetal alcohol spectrum disorders.

Introduction

Exposure to ethanol during pregnancy causes fetal alcohol spectrum disorders (FASDs), a major public health problem with an estimated prevalence as high as 2–5% in the United States and several Western European countries (May et al., 2009). FASD is one of the main causes of intellectual disability in Western nations (Mattson et al., 2011) and is accompanied by widespread neuropsychological deficits, such as verbal learning/recall abilities (Mattson and Riley, 1998; Mattson et al., 1998), including deficits in learning and memory (Goodman et al., 1999; Mattson et al., 1999). During the third trimester of human gestation, the brain undergoes a stage of rapid growth (Bayer et al., 1993) and is particularly sensitive to ethanol; thus, binge models have been established to examine the effects of ethanol consumption on fetal brain development in humans (Gil-Mohapel et al., 2010). A single day of ethanol intoxication at postnatal day 7 (P7) triggers a massive wave of neurodegeneration (Ikonomidou et al., 2000b; Subbanna et al., 2013) and persistent synaptic and memory deficits in adult mice (Izumi et al., 2005; Wilson et al., 2011; Sadrian et al., 2012).

A strong interaction has been elucidated between ethanol and the molecular constituents of endocannabinoid (EC) system (for review, see Basavarajappa, 2007c; Pava and Woodward, 2012), which includes endogenous ligands (ECs), receptors, as well as synthesizing and degrading enzymes (Piomelli, 2003; Basavarajappa, 2007d). An emerging body of research has revealed multiple ways in which the EC system plays an important role in regulating synaptic events (Ohno-Shosaku et al., 2001; Wilson and Nicoll, 2001; Bacci et al., 2004) in the developing and adult brain (Basavarajappa et al., 2009).

The cannabinoid receptor type 1 (CB_1R) is one of the most abundant inhibitory G-protein-coupled receptors expressed in the brain (Howlett et al., 1986; Herkenham et al., 1990). Activation of CB_1Rs also prevents the recruitment of new synapses by inhibiting the formation of cAMP (Kim and Thayer, 2001). Al-

Received Aug. 8, 2012; revised Jan. 24, 2013; accepted Feb. 25, 2013.

Author contributions: B.S.B. designed research; S.S., M.S., D.P., S.X., and B.S.B. performed research; B.S.B. analyzed data; B.S.B. wrote the paper.

This work was supported by National Institutes of Health/National Institute on Alcohol Abuse and Alcoholism Grants AA11031 and AA019443 (B.S.B.). D.P. was supported by National Institute on Drug Abuse Award 5F32DA21977.

The authors declare no competing financial interests.

Correspondence should be addressed to Balapal S. Basavarajappa, Division of Analytical Psychopharmacology, Nathan Kline Institute for Psychiatric Research, 140 Old Orangeburg Road, Orangeburg, NY 10962. E-mail: basavaraj@nki.rfmh.org.

DOI:10.1523/JNEUROSCI.3786-12.2013

 0270-6474/13/336350-17$15.00/0

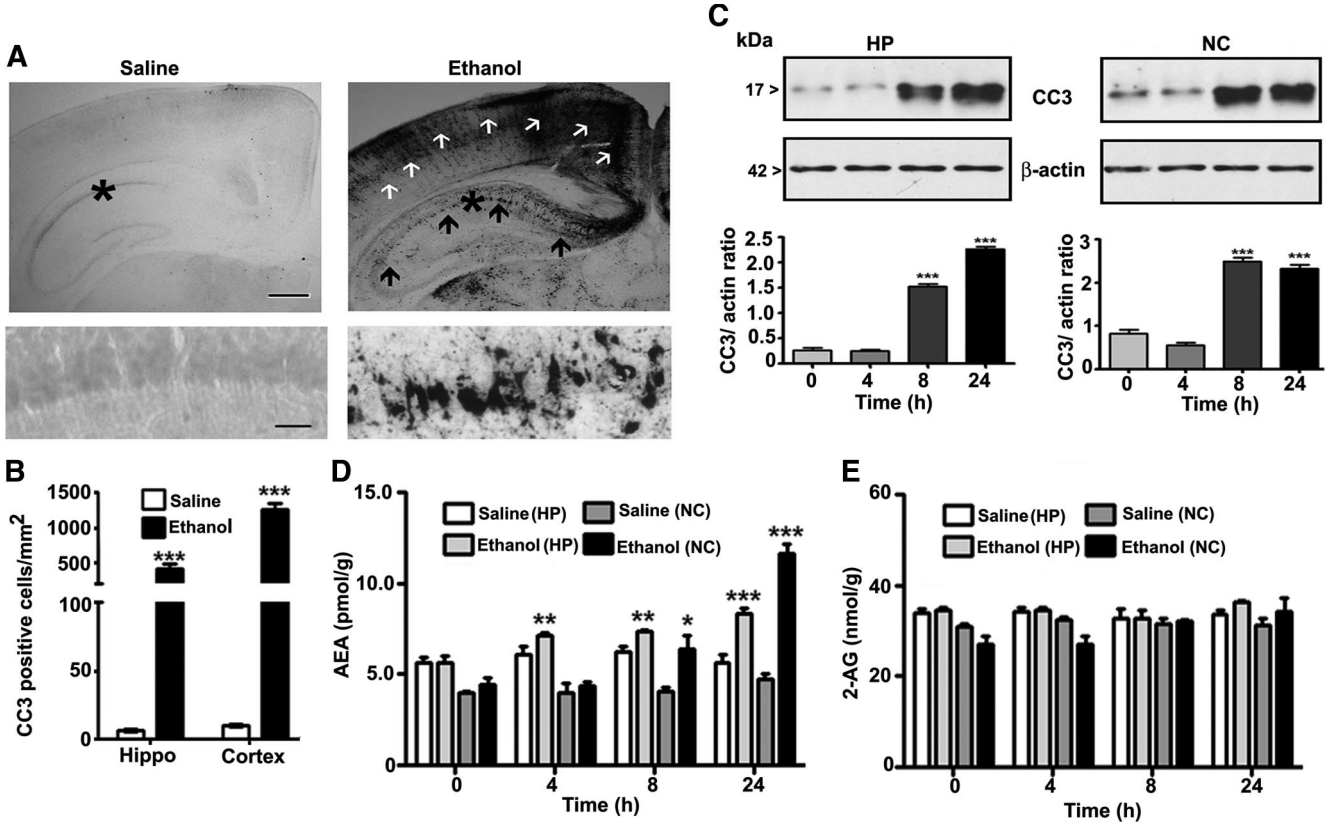

Figure 1. Ethanol induces apoptotic neurodegeneration and enhances AEA but not 2-AG levels in the P7 mouse brain. ***A***, Coronal brain sections exposed to saline and ethanol were immunostained with an anti-CC3 antibody. The black and white arrows show the CC3-positive neurons in the hippocampus and neocortex regions, respectively. The respective images were enlarged to show CC3-positive cells (*). Scale bars: top, 200 μm; bottom, 50 μm. ***B***, CC3-positive cells were counted in the hippocampus and the retrosplenial neocortex ($n = 10$ pups per group) (***$p < 0.001$). ***C***, Western blot analysis of CC3 using hippocampal and cortical (cytosolic) extracts (20 μg) from saline- and ethanol-treated groups ($n = 10–15$ pups per group). The graphs represent the ratio of the proteins normalized to β-actin (***$p < 0.001$). ***D***, ***E***, The total extracts were subjected to LC-MS analysis of the AEA (***D***) and 2-AG (***E***) contents in the hippocampus and neocortex ($n = 10–15$ pups per group) (compared with the saline-treated group) (*$p < 0.05$, **$p < 0.01$, ***$p < 0.001$). All the statistical analyses were done using one-way ANOVA with Bonferroni's *post hoc* tests. The error bars represent the SEM. HP, Hippocampus; NC, neocortex.

though the intracellular signaling events involving mitogen-activated protein kinase (MAPK) coupled to the activation of CB_1Rs are limited (Berghuis et al., 2007) or not known during postnatal development, several studies using cell lines suggest both upregulation and downregulation of the MAPK in Δ^9-tetrahydrocannabinol-mediated apoptosis (De Petrocellis et al., 1998; Galve-Roperh et al., 2000). Moreover, cannabis use during brain development induces several specific human developmental disorders (Stefanis et al., 2004), including fetal alcohol syndrome-like deficits (Wu et al., 2011), which is likely mediated through the activation of CB_1Rs.

Furthermore, a CB_1R agonist combined with a low concentration of ethanol has been shown to enhance the susceptibility of the neonatal brain to neurodegeneration, which is consistent with observations for a high concentration of ethanol alone (Hansen et al., 2008). The activation of EC–CB_1R-mediated signaling is a potential mechanism by which ethanol may alter early brain development and may be an important candidate for the pathophysiology of FASD. For the first time, we report that P7 ethanol treatment increased anandamide (AEA)/CB_1R signaling and resulted in neonatal neurodegeneration and contributes to the development of synaptic and memory deficits relevant to FASD.

Materials and Methods

Animals and treatment. C57BL/6J mice or CB_1R wild-type (WT) and knock-out (KO) mice on C57BL/6J background were housed in groups under standard laboratory conditions (12 h light/dark cycle) with food and water available *ad libitum*. Animal care and handling procedures followed Nathan Kline Institute Institutional Animal Care and Use Committee and National Institutes of Health guidelines. The genotype of CB_1R WT and KO mice was determined by PCR of genomic DNA obtained from mouse tails as described previously (Basavarajappa et al., 2003). An ethanol treatment paradigm, which has been shown previously to induce robust apoptotic neurodegeneration in P7 mice (Olney et al., 2002), was used in the current study. Half of the pups (male and female) in each litter were treated subcutaneously with saline and the other half with ethanol at P7 (based on the day of birth) (2.5 g/kg, sc at 0 h and again at 2 h) as described previously by our laboratory (Wilson et al., 2011; Sadrian et al., 2012; Subbanna et al., 2013). For blood ethanol levels, pups were killed by decapitation; truncal blood was collected at 3 and 9 h after the second ethanol injection. The concentrations of ethanol in pup serum were then determined using a standard alcohol dehydrogenase-based method (Lundquist, 1959). For the SR141716A [*N*-piperidino-5-(4-chlorophenyl)-1-(2,4-dichlorophenyl)-4-methyl-3-pyrazole carboxamide] (SR) experiments, SR (gift from RBI) was dissolved in 10 μl of ethanol followed by a few drops of Tween 80, and then volume was made up with sterile saline solution. The SR solution was administered (0.25, 0.5, and 1 mg/kg, sc) at a volume of 5 μl/g body weight 30 min before ethanol administration. The SR vehicle solution was injected as a control. In some experiments, we injected (subcutaneously) P7 CB_1R WT and KO mice with NMDA receptor antagonist MK-801 (1 mg/kg, prepared as described for SR). Mice were kept with the dams until the pups were killed, and their brains were removed 4–24 h or 90 d after the first saline/ethanol injection. The brains were processed for several analyses, as described below. Four to 15 animals were used for each data point.

Measurement of AEA and 2-arachidonoylglycerol levels by liquid chromatography mass spectrometry. AEA and 2-arachidonoylglycerol (2-AG) levels in hippocampal and cortical tissue extracts were measured by a liquid chromatography mass spectrometry (LC-MS) method using the isotopic dilution procedure as described previously (Vinod et al., 2005) with minor modifications. Briefly, tissue (hippocampus and cortex) was homogenized in chloroform/methanol/Tris buffer (2:1:1), pH 7.4, containing 0.25 mM PMSF, 1% butylated hydroxytoluene, 50 ng of AEA-d8, and 500 ng of 2-AG-d8. The homogenate was centrifuged, and the organic layer was dried under nitrogen. The residue was dissolved in 0.3 ml of ethyl acetate and centrifuged. The supernatant was dried under nitrogen. The residue was dissolved in ethanol (30 μl) and used for the measurement of AEA and 2-AG by LC-MS (Agilent 1100 series mass LC-MSD). The separation was achieved on a SUPELCOSIL LC-8 column (25 cm × 4.6 mm, 5 mm) using methanol/ammonium acetate/acetic acid (85:15:0.05) as a mobile phase. The standard curve was fitted with a quadratic equation with the curve encompassing a range of 0.5–50 ng for AEA and 50–2500 ng for 2-AG and was processed similarly with quality controls with brain tissue extracts.

Immunohistochemistry. Previous studies indicate that the maximum caspase-3 activation (in one or more brain regions) was induced between 8 and 24 h after the first ethanol injection (Ikonomidou et al., 2000b; Wilson et al., 2011). Therefore, 8 or 18 h after the first ethanol/saline injection, the pups were anesthetized with isoflurane and perfused with a solution containing 4% paraformaldehyde and 4% sucrose in 0.05 M cacodylate buffer, pH 7.2, and the brains were further processed according to our previously described protocols (Wilson et al., 2011). Briefly, the free-floating sections obtained from ethanol- and saline-exposed brains (8 h of exposure) were immunostained using anti-rabbit cleaved caspase-3 (Asp175) (CC3) (1:1000, catalog #9661; Cell Signaling Technology) by the ABC reagents (Vectastain ABC Elite Kit; Vector Laboratories) with a peroxidase substrate (DAB) kit (Vector Laboratories). The primary antibodies were omitted from the reactions as a control for secondary antibody specificity. Also, preincubation with blocking peptides for the anti-rabbit CC3 (Cell Signaling Technology) completely blocked the immunostaining of these antibodies. The free-floating sections obtained from ethanol- and saline-exposed brains (18 h of exposure) were processed for Fluoro-Jade (F-J) (Millipore) staining and quantified as described previously (Wilson et al., 2011). All photomicrographs were taken through a 5×, 10×, or 40× objective with a Nikon Eclipse TE2000 inverted microscope attached to a digital camera (DXM1200F; Morrell Instrument Company).

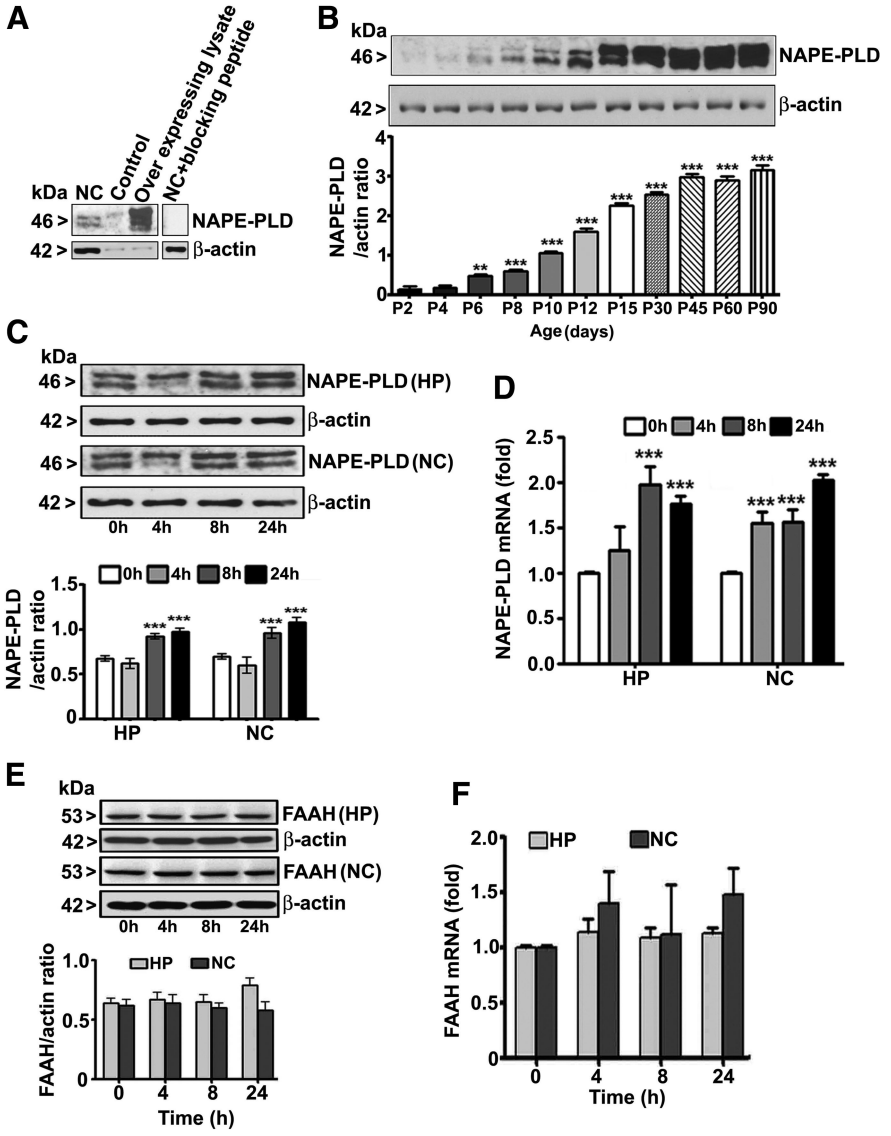

Figure 2. Expression of NAPE–PLD during mouse brain development and the influence of ethanol on NAPE–PLD and FAAH levels in P7 mice. ***A***, Western blot analysis of NAPE–PLD expression in neocortex extract (NC, lane 1) (10 μg), control vector transfected HEK293T cells lysates (lane 2) (2.0 μg), NAPE–PLD over expressing lysates (lane 2) (2.0 μg), and neocortex extract (10 μg) with NAPE–PLD blocking peptide (lane 4). ***B***, Western blot analysis of NAPE–PLD expression using neocortical total extracts. The representative blot shows the developmental changes in NAPE–PLD expression ($n = 8$ pups per group) (compared with the P2 group) (**$p < 0.01$, ***$p < 0.001$). ***C***, A Western blot analysis of NAPE–PLD and β-actin (loading control) in the hippocampal and neocortical extracts from the saline- and ethanol-treated groups (***$p < 0.001$). ***D***, A qPCR analysis of NAPE–PLD mRNA in the hippocampal and cortical total extracts from the saline- and ethanol-treated groups ($n = 15$ pups per group) (**$p < 0.01$, ***$p < 0.001$) (compared with the 0.0 control group). ***E***, Western blot analysis of FAAH and β-actin (loading control) in hippocampal and neocortex extracts from the saline- and ethanol-treated groups ($p > 0.05$). ***F***, A qPCR analysis of FAAH mRNA in the hippocampal and cortical total extracts from the saline- and ethanol-treated groups ($n = 8$ pups per group) (compared with the 0.0 control group) ($p > 0.05$). Statistical analysis was done using one-way ANOVA with Bonferroni's *post hoc* tests. The error bars represent the SEM. HP, Hippocampus; NC, neocortex.

Electrophoresis and immunoblot. For Western blot analysis, 4–24 h after the first saline or ethanol injection, pups were killed by decapitation, and cortex and hippocampus were dissected, flash frozen, and stored at −80°C. Homogenates from the hippocampus and neocortex of the pups were processed as described previously (Lubin and Sweatt, 2007). Tissue homogenates containing freshly added 1% protease inhibitor mixture (Roche) and phosphatase inhibitors were centrifuged at 7700 × *g* for 1 min, and the supernatant (total extract) was aspirated. The membrane and cytosolic fractions were prepared from the total extract as described previously (Basavarajappa and Hungund, 2001) and stored at −80°C until use. The samples were prepared in a sample buffer as described previously by our laboratory (Basavarajappa et al., 2008). The blots were incubated in primary antibody: anti-rabbit CC3 (1:1000), anti-mouse-cTau (1:5000, catalog #27027; EMD Millipore), anti-rabbit NAPE–PLD (4 μg/ml, catalog #10305; Cayman Chemicals), anti-rabbit CB_1R (0.1 μg/ml; Thermo Fisher Scientific), anti-rabbit fatty acid amide hydrolase (FAAH) (1:1000, catalog #101600; Cayman Chemicals), anti-rabbit glycerophosphodiesterase (GDE1) (1:1000, L-25, sc-133615; Santa

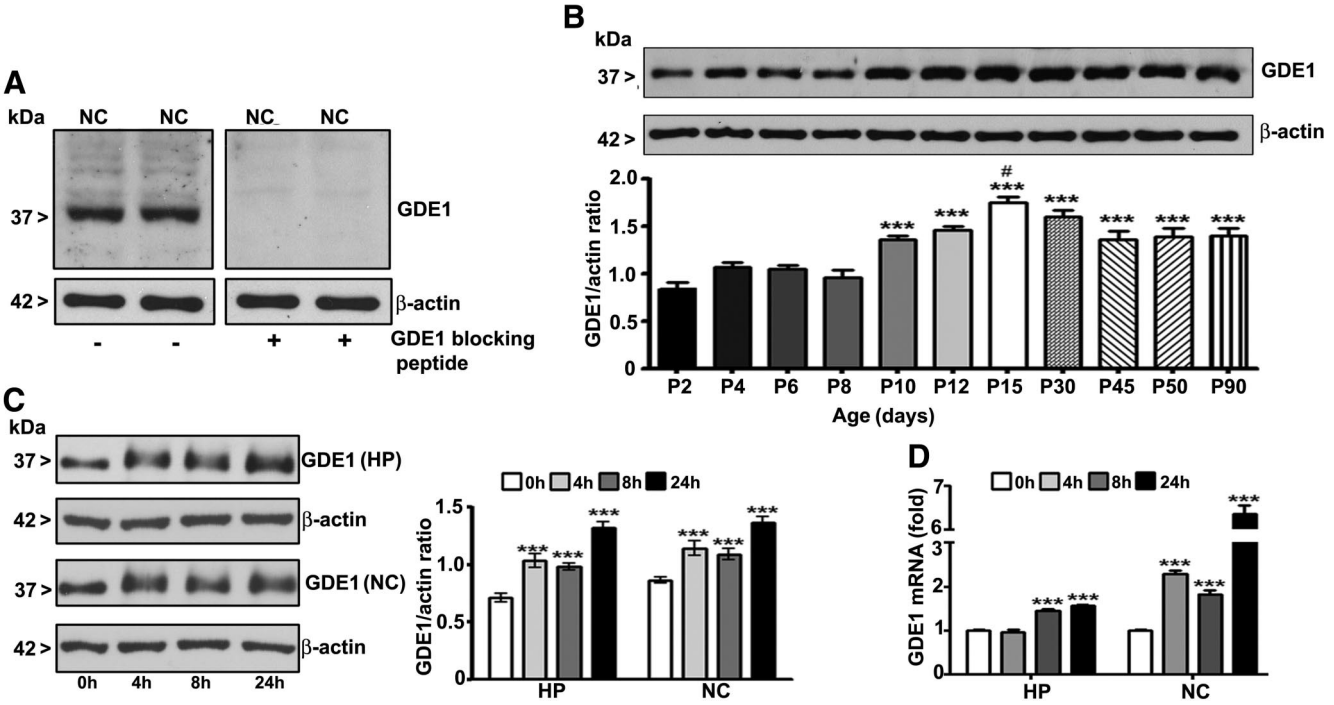

Figure 3. Developmental pattern and the influence of ethanol on GDE1 expression in P7 mice. ***A***, Western blot analysis of GDE1 expression in neocortex extract (NC) (10 μg) and with GDE1 blocking peptide. ***B***, Western blot analysis of GDE1 expression using neocortical total extracts. The representative blot shows the developmental changes in GDE1 protein expression ($n = 8$ pups pr group) (***$p < 0.001$, compared with the P2 group; $^{\#}p < 0.01$, compared with the P90 group). ***C***, A Western blot analysis of GDE1 and β-actin (loading control) in the hippocampal and neocortical extracts from the saline- and ethanol-treated groups (***$p < 0.001$). ***D***, A qPCR analysis of GDE1 mRNA in the hippocampal and neocortical total extracts from the saline- and ethanol-treated groups ($n = 15$ pups per group) (compared with the 0.0 control group) (***$p < 0.001$). Statistical analysis was done using one-way ANOVA with Bonferroni's *post hoc* tests. The error bars represent the SEM. HP, Hippocampus; NC, neocortex.

Cruz Biotechnology), anti-rabbit p44/42 MAPK (ERK1/2) (1:500, catalog #9102; Cell Signaling Technology), anti-rabbit phospho-p44/42 MAPK (1:1000, catalog #9101; Cell Signaling Technology), anti-rabbit pAKT (1:000, catalog #9275; Cell Signaling Technology), anti-rabbit AKT (1:1000, catalog #9272; Cell Signaling Technology), and anti-mouse β-actin (1:5000, catalog #ab24701; Abcam) for 3 h at room temperature or overnight at 4°C and processed as previously described by our laboratory (Basavarajappa et al., 2008). Incubation of blots with a secondary antibody (goat anti-mouse peroxidase conjugate, #AP 124P, 1:5000; goat anti-rabbit, #AP132P, 1:5000; Millipore) alone did not produce any bands.

Real-time quantitative PCR. For the quantitative PCR (qPCR) studies, 4–24 h after the first saline or ethanol injection, the hippocampus and cortex of the pups were subjected to a total RNA preparation using the RNeasy mini kit (Qiagen). The mRNA was reverse transcribed into cDNA using the Maxima First Strand cDNA Synthesis Kit from Fermentas on a programmable thermal cycler (PCR-Sprint; Thermo Fisher Scientific). qPCR for NAPE–PLD, Gde1, Faah, and Cb1r was performed with the integrated thermocycler and fluorescence detector ABI PRISM 7900HT Sequence Detector (Applied Biosystems) using the TaqMan Gene Expression Assays Mm00724596_m1 (NAPE–PLD), Mm00450997_m1 (Gde1), Mm00515684_m1 (Faah), Mm01212171_s1 (Cb1r), and 4352932 (Gapdh) (Applied Biosystems). GAPDH was used as an endogenous mRNA control. Three independent runs were performed for each set of samples. For each run, triplicate reactions were performed for each sample. Data obtained were analyzed with the use of SDS2.4 software (Applied Biosystems). The amount of target (NAPE–PLD, Gde1, Faah, and Cb1r), normalized to endogenous reference (Gapdh) and relative to a calibrator, was given by-2ΔΔCt (for detailed reference on qPCR procedure, see Psychoyos et al., 2012).

Long-term potentiation. Three-month-old male and female mice ($n = 5$ per group) treated with saline–vehicle, ethanol–vehicle, SR, ethanol + SR, and CB_1R WT and KO with and without ethanol at P7 were killed by cervical dislocation followed by decapitation. Hippocampi were quickly removed. Transverse hippocampal slices (400 μm) were cut and recorded according to standard procedures (Vitolo et al., 2002; Sadrian et al., 2012). After cutting, hippocampal slices were transferred to a recording chamber in which they were maintained at 29°C and perfused with artificial CSF (ACSF) continuously bubbled with 95% O_2 and 5% CO_2. The ACSF composition was the following (in mM): 124.0 NaCl, 4.4 KCl, 1.0 Na_2HPO_4, 25.0 $NaHCO_3$, 2.0 $CaCl_2$, 2.0 $MgSO_4$, and 10.0 glucose (290–300 osmolarity). CA1 field EPSPs (fEPSPs) were recorded by placing both the stimulating and the recording electrodes in CA1 stratum radiatum. Basal synaptic transmission was assayed by plotting the stimulus voltages against slopes of fEPSP. For long-term potentiation (LTP) experiments, a 10 min baseline was recorded every minute at an intensity that evokes a response ~35% of the maximum evoked response. LTP was induced using theta-burst stimulation (four pulses at 100 Hz, with the bursts repeated at 5 Hz, and each tetanus including 3 × 10 burst trains separated by 15 s). Responses were recorded for 2 h and measured as fEPSP slope expressed as percentage of baseline. The results were expressed as mean ± SEM.

Novel object recognition memory. Novel object recognition memory (ORM) was evaluated as described previously (Ennaceur and Delacour, 1988), which is based on the natural tendency of rodents to explore a novel object more than a familiar one. It is a pure working memory (Alexinsky and Chapoutier, 1978) and not based on usual positive or negative reinforcers, such as food or electric shocks that make the interpretation of the effects of brain modification on memory deficit (Huston et al., 1974; Ketty, 1976; Jaffard et al., 1981; Gaffan et al., 1984). The ORM was performed in a 40 × 40 cm open field surrounded by 35-cm-high walls made of Plexiglas (Stoelting). Three- to 4-month-old male mice ($n = 8$ per group) treated with saline–vehicle, ethanol–vehicle, SR, ethanol + SR, and CB_1R WT and KO with and without ethanol at P7 were submitted to a habituation session in which they were allowed to freely explore the open field for 5 min twice for 2 d. No objects were placed in the box during the habituation trial. Twenty-four hours after habituation, training (T1) was conducted by placing individual mice for 3 min in the open field, in which two identical objects (objects a1 and a2) were

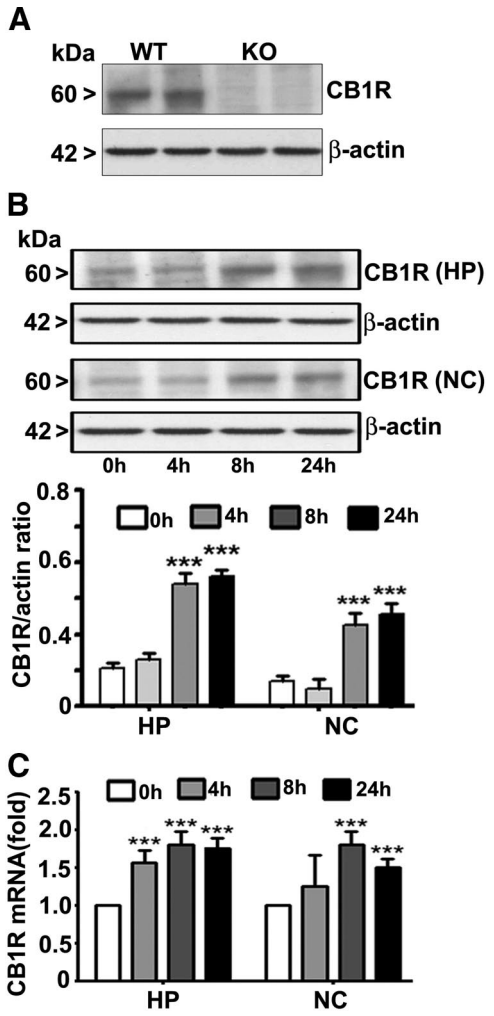

Figure 4. Ethanol enhances the expression of CB_1Rs in the neonatal brain. ***A***, Western blot analysis of CB_1R expression in WT and KO brain neocortical extracts. ***B***, Western blot analysis of CB_1R expression in hippocampal and neocortical membrane fractions from the saline- or ethanol-treated groups; β-actin was used as a loading control ($n = 15$ pups per group) (***$p < 0.001$, compared with the saline-treated control group). ***C***, A qPCR analysis of CB_1R mRNA in hippocampal and cortical total extracts from the saline- and ethanol-treated groups ($n = 8$ pups per group) (***$p < 0.001$, compared with the 0.0 control group). Statistical analysis was done using one-way ANOVA with Bonferroni's *post hoc* tests. The error bars represent the SEM. HP, Hippocampus; NC, neocortex.

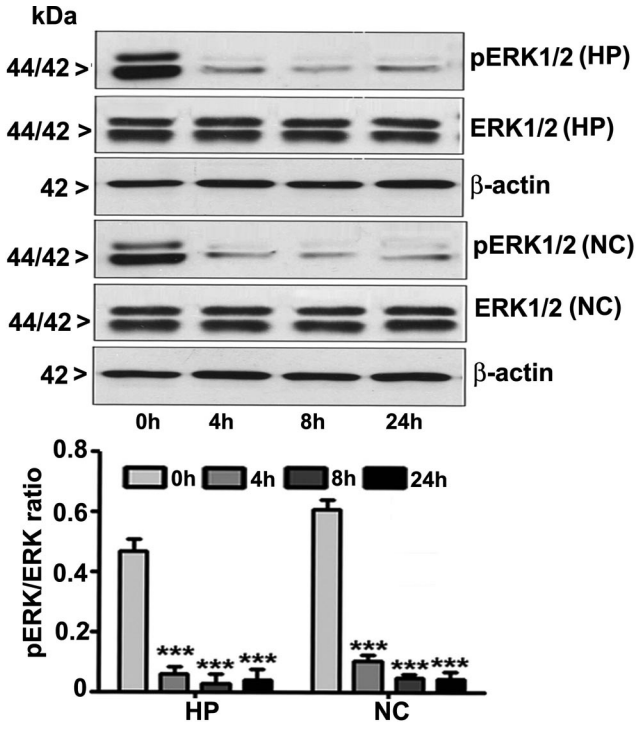

Figure 5. Ethanol inhibits ERK1/2 phosphorylation in the neonatal brain. A Western blot analysis of pERK1/2 and ERK1/2 in hippocampal and cortical cytosolic extracts from the saline- or ethanol-treated groups; β-actin was used as a loading control ($n = 10$ pups per group) (***$p < 0.001$, compared with the saline control group). Statistical analysis was done using one-way ANOVA with Bonferroni's *post hoc* tests. The error bars represent the SEM. HP, Hippocampus; NC, neocortex.

positioned in two adjacent corners at 10 cm from the walls. In a short-term recognition memory test given at 1 and 4 h (retention) after the training (T2), the mice explored the open field for 3 min in the presence of one familiar (a1) and one novel (b1, 1 h; b2, 4 h) object. In a long-term recognition memory test given at 24 h (retention) after training (T2), the mice explored the open field for 3 min in the presence of one familiar (a1) and one novel (b3; different from b1 and b2) object. All combinations and locations (left and right) of the objects were used in a balanced manner to reduce potential biases attributable to preferences for particular locations or objects. All objects had similar textures and sizes but had distinctive shapes and colors (Stoelting). Between trials, the objects were washed with 10% ethanol solution. Exploration was defined as directing the nose to the object at a distance of no more than 2 cm and/or touching the object with the nose. Sitting on the object was not considered as exploratory behavior. e1 and e2 are measures of the total exploration time of both objects during T1 and T2 (1, 4, and 24 h), respectively. d2 was considered as index measures of discrimination between the new and the familiar objects. d2 is a relative measure of discrimination that corrects the difference between exploring the familiar and the novel object for exploration activity (e2) and appears to be independent of the total exploration times (Sik et al., 2003). The times spent exploring each object during T1 and T2 were recorded manually with a personal computer. The data were expressed as mean ± SEM.

Statistical analyses. Unless indicated otherwise, the experiments were performed in triplicate using equal number of animals per treatment. All of the data are presented as the mean ± SEM. A statistical comparison of the data was performed by either a one-way ANOVA or a two-way ANOVA with Bonferroni's *post hoc* test. In all of the comparisons, $p < 0.05$ was considered to indicate statistical significance. The statistical analyses were performed using the Prism software version 5 (GraphPad Software).

Results

Enhanced AEA contents during ethanol-induced neurodegeneration in the developing brain

To gain insight into EC-mediated events during P7 ethanol-induced neurodegeneration, we first examined the effects of ethanol exposure on neurodegeneration, EC levels, and enzymes responsible for the synthesis and degradation of AEA and CB_1Rs levels in the hippocampus and neocortex, two brain regions (Olney et al., 2002) that are affected by ethanol treatment in P7 mouse pups. These analyses were performed after the administration of ethanol (2.5 g/kg, sc at 0 h and again at 2 h) to mouse pups at P7. This experimental paradigm resulted in a blood alcohol level (BAL) of ~0.49 ± 0.3 g/dl at 3 h that was gradually reduced to 0.28 ± 0.09 g/dl at 9 h.

This ethanol paradigm produced a widespread pattern of neurodegeneration throughout the forebrain (Fig. 1*A*) [hippocampus ($F_{(1,11)} = 90, p < 0.001$) and cortex ($F_{(1,11)} = 750, p < 0.001$) regions] (one-way ANOVA), as indicated by caspase-3 activation (formation of CC3) in ethanol-exposed brains (Fig. 1*B*). Subsequently, we also evaluated for neurodegeneration in hippocampal

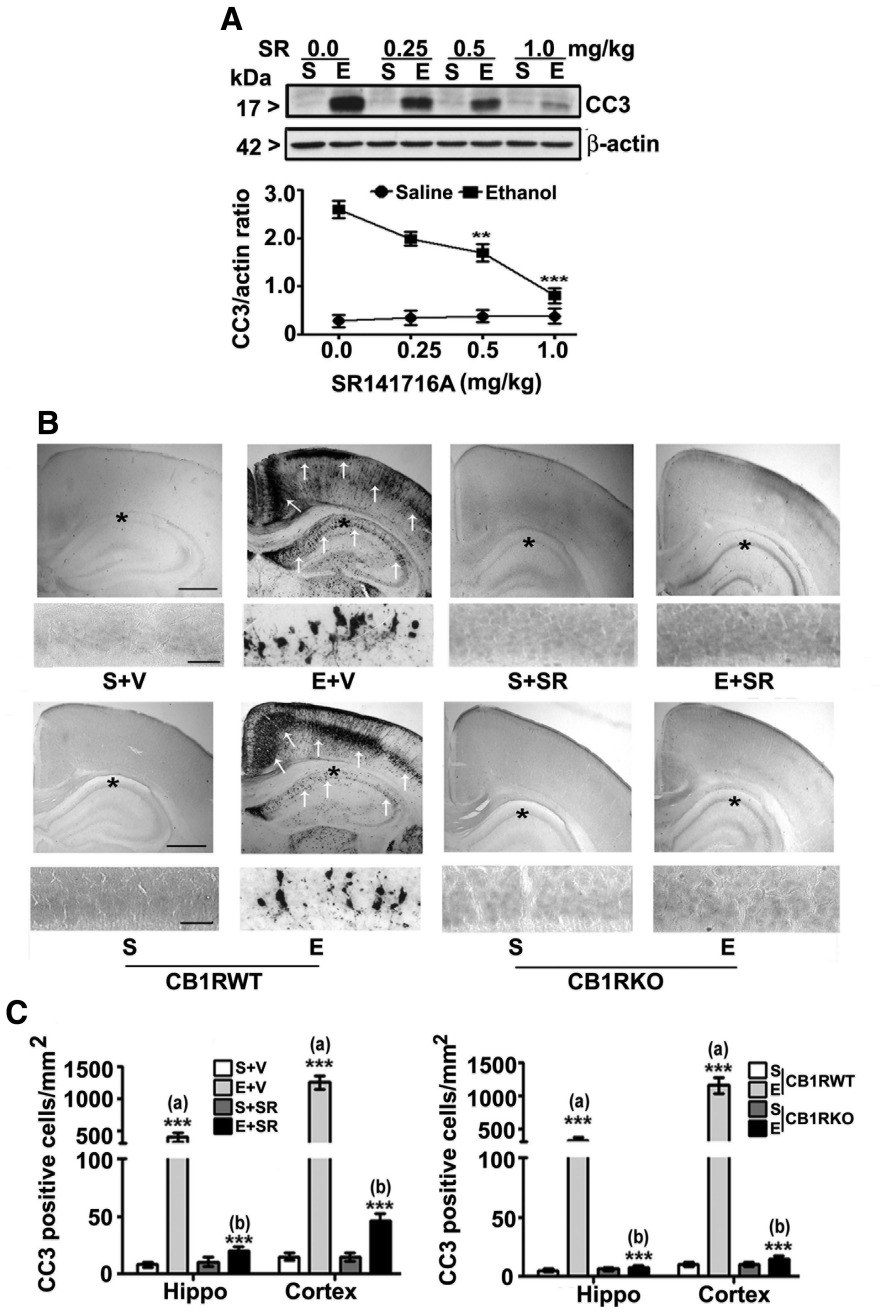

Figure 6. Pharmacological inhibition or genetic deletion of CB_1Rs provides protection against ethanol-induced activation of caspase-3 in the neonatal mouse brain. ***A***, Mice pretreated for 30 min with various doses of SR (0, 0.25, 0.5, and 1 mg/kg) or vehicle were exposed to ethanol, and CC3 levels were determined by a Western blot analysis (**$p < 0.01$, ***$p < 0.001$). ***B***, Mice pretreated (30 min) with SR (1 mg/kg) or vehicle were exposed to ethanol and were perfusion fixed 8 h after treatment, and the brain sections from the four treatment groups [saline + vehicle (S+V), ethanol + vehicle (E+V), saline + SR (S+SR), and ethanol + SR (E+SR)] and the CB_1R WT and KO mice with and without P7 ethanol were stained with the CC3 antibody. The representative images show the retrosplenial cortex and hippocampus. The white arrows denote the CC3-positive neurons in the hippocampus and cortex. The respective images were enlarged to show CC3-positive cells (*). ***C***, CC3-positive cells were counted in the hippocampus and the retrosplenial cortex from all the treatment groups ($n = 15$ pups per group) (***$p < 0.001$). Statistical analysis was calculated using two- and one-way ANOVA with Bonferroni's *post hoc* tests (in one-way ANOVA, the comparison was performed between S+V vs E+V and E+V vs E+ SR). Error bars indicate SEM. (a), Compared with respective saline control; (b), compared with respective ethanol group in all the bar graphs. Scale bars: top, 200 μm; bottom, 50 μm.

and neocortical protein extracts by Western blot analysis. Comparisons using one-way ANOVA with Bonferroni's *post hoc* tests indicate that the saline and 4 h ethanol treatment groups were not significantly different, whereas the 8 and 24 h ethanol groups exhibited significantly greater proportions of neuronal death in both the hippocampus ($F_{(3,28)} = 75, p < 0.0001$) and neocortex ($F_{(3,28)} = 80, p < 0.001$) (Fig. 1*C*). Together, our experimental conditions recapitulated the apoptotic patterns and severity described for this ethanol treatment paradigm in the developing brain (Ikonomidou et al., 2000b; Olney et al., 2002).

We tested the potential changes in EC levels attributable to ethanol treatment in a condition that induces widespread apoptotic neurodegeneration. We evaluated the EC levels using an LC-MS method at several time points after ethanol treatment. Comparisons using one-way ANOVA with Bonferroni's *post hoc* tests demonstrated that AEA levels were enhanced by ethanol in a time-dependent manner in the hippocampus ($F_{(3,20)} = 29, p < 0.001$) and neocortex ($F_{(3,20)} = 60, p < 0.001$) (Fig. 1*D*) compared with saline. However, no significant net changes in the 2-AG levels (Fig. 1*E*) ($p > 0.05$) were observed. Therefore, we concluded that AEA levels are enhanced after ethanol exposure in neonatal mice.

Ethanol exposure at P7 enhances NAPE–PLD and GDE1 enzymes involved in AEA formation

To examine the mechanism by which ethanol may enhances AEA levels, we measured the levels of NAPE–PLD, an enzyme involved in AEA biosynthesis (Basavarajappa, 2007a). First, we characterized the antibody specificity using NAPE–PLD over expressing lysates (Fig. 2*A*, lane 3) along with control (Fig. 2*A*, lane 2) and brain extracts (neocortex) (Fig. 2*A*, lane 1). In addition, Western blotting with anti-NAPE–PLD antibodies preabsorbed with blocking peptide (catalog #10303; Cayman Chemicals) also confirmed the specificity of this antibody in the developing neocortex tissues (Fig. 2*A*, lane 4). This antibody recognized a major band (doublet) at 46 kDa corresponding to NAPE–PLD protein (Morishita et al., 2005). To identify the patterns of NAPE–PLD protein expression during mouse brain development, protein extracts from mouse brain neocortical tissues at several developmental stages were examined by Western blot analysis. NAPE–PLD protein levels were significantly lower during the synaptogenic period of brain development ($F_{(10,55)} = 274, p < 0.001$) (Fig. 2*B*) and gradually increased to adult levels. Consistent with previous studies (Guo et al., 2011; Jacob et al., 2011), the levels of the housekeeping protein actin did not change significantly during the various stages of brain development. These findings are consistent with the patterns of NAPE–PLD expression during brain development (Morishita et al., 2005). To examine the influence of ethanol exposure on the NAPE–PLD levels, we mea-

sured the NAPE–PLD protein levels in hippocampal and neocortical extracts by Western blot. These results demonstrated that, compared with the control, ethanol increased the NAPE–PLD protein levels in the hippocampus ($F_{(3,20)} = 11, p < 0.001$) and neocortex ($F_{(3,20)} = 22, p < 0.0001$) (Fig. 2*C*) at 8 and 24 h. These findings are consistent with the enhanced AEA levels observed in the same brain regions. We next examined whether the increased NAPE–PLD protein is attributable to enhanced NAPE–PLD gene transcriptional activity. Our results suggest that ethanol enhanced the NAPE–PLD mRNA levels in the hippocampus ($F_{(3,28)} = 9, p < 0.001$) at 8 and 24 h and the neocortex ($F_{(3,28)} = 19, p < 0.001$) (Fig. 2*D*) at all of the time points measured. Additional experiments were performed to determine whether ethanol affects the AEA hydrolyzing enzyme FAAH. It was shown previously that the FAAH distribution during postnatal development was very similar to the adult pattern (Morozov et al., 2004). Our results suggest that ethanol did not considerably alter either the FAAH protein (Fig. 2*E*) or the mRNA levels (Fig. 2*F*) in the hippocampus or neocortex ($p > 0.05$). Together, it appears that ethanol enhances AEA levels through the transcriptional activation of the NAPE–PLD gene and protein expression in the developing brain. Overwhelming data suggest that lack of NAPE–PLD significantly reduces the levels of AEA and N-acylethanolamine (NAE) (Nyilas et al., 2008; Tsuboi et al., 2011) in the brain, although some controversy exists whether NAPE–PLD contributes to the formation of AEA in the brain (Leung et al., 2006). Interestingly, a recent study suggests significant reductions in the accumulation of brain NAEs, including AEA, in GDE1/NAPE–PLD double KO mice treated with an FAAH inhibitor that blocks NAE degradation (Simon and Cravatt, 2010).

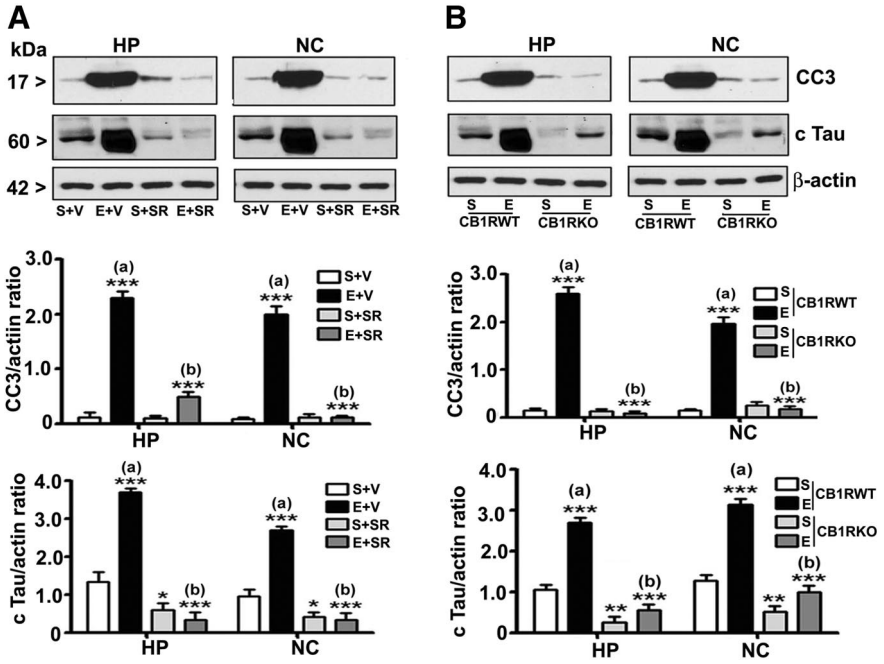

Figure 7. SR pretreatment or genetic deletion of CB_1Rs prevents ethanol-induced generation of CC3 and cTau in the neonatal mouse brain. ***A***, Mice pretreated (30 min) with SR (1 mg/kg) or vehicle were exposed to ethanol. Cytosolic extracts from the four treatment (8 h) groups [saline + vehicle (S+V), ethanol + vehicle (E+V), saline + SR (S+SR), and ethanol + SR (E+SR)] were collected and processed for a Western blot to analyze the levels of CC3 and cTau (*$p < 0.05$, **$p < 0.01$, ***$p < 0.001$). ***B***, In addition, similar analyses were also performed using CB_1R WT and KO P7 mice (**$p < 0.01$, ***$p < 0.001$). Representative blots are shown for the hippocampal and cortical cytosolic extracts ($n = 10–15$ pups per group). Statistical analysis was done using two-way ANOVA with Bonferroni's *post hoc* tests. The error bars represent the SEM. (a), Compared with respective saline control; (b), compared with respective ethanol; (c), compared with saline group in all the bar graphs. HP, Hippocampus; NC, neocortex.

Thus, we examined the influence of ethanol exposure on the GDE1 levels. Western blotting with anti-GDE1 antibodies preabsorbed with blocking peptide confirmed the specificity of this antibody in the developing neocortex tissues. GDE1 blocking peptide (L-25, sc-133615PS; Santa Cruz Biotechnology) blocked a major band corresponding to 37 kDa specific for GDE1 protein (Fig. 3*A*). To identify the patterns of GDE1 protein expression during mouse brain development, protein extracts from mouse brain neocortical tissues at several developmental stages were examined by Western blot analysis. GDE1 protein levels were lower during P2–P8 stage, significantly increased during P10–P15, and stabilized during P30–P90 developmental stages ($F_{(10,55)} = 17, p < 0.001$) (Fig. 3*B*). In fact, P15 ($^{\#}p < 0.01$) has higher levels of GDE1 compared with P2 or P90 mice. Consistent with previous studies (Guo et al., 2011; Jacob et al., 2011), the levels of the housekeeping protein actin did not change significantly during the various stages of brain development. To examine the influence of ethanol exposure on the GDE1 levels, we measured the GDE1 protein levels in hippocampal and neocortical extracts by Western blot. Our findings demonstrate that, compared with the control, ethanol increased the GDE1 protein levels in the hippocampus ($F_{(3,20)} = 28, p < 0.001$) and neocortex ($F_{(3,20)} = 17, p < 0.0001$) (Fig. 3*C*) at all of the time points measured. We next examined whether the increased GDE1 protein is attributable to enhanced GDE1 gene transcriptional activity. Our results suggest that ethanol enhanced the GDE1mRNA levels in the hippocampus ($F_{(3,28)} = 26, p < 0.001$) at 8 and 24 h and neocortex ($F_{(3,28)} = 18, p < 0.001$) (Fig. 3*D*) at all of the time points measured. Thus, combined increase in GDE1 and NAPE–PLD protein levels may be responsible for enhanced AEA levels found in the developing brain exposed to ethanol.

Increased CB_1R expression after ethanol exposure in neonatal mice

Previous human fetal studies indicate the presence of CB_1Rs at 19 weeks of gestation that are functionally coupled to signal transduction mechanisms from early prenatal stages (Mato et al., 2003). Similar functional CB_1Rs have been detected in the developing rat brain even 1 week before the end of gestation. The cellular and subcellular patterns of CB_1R expression during early postnatal life are similar to the adult patterns (Morozov and Freund, 2003). These observations suggest a specific role for the CB_1R in the events related to neural development. We characterized the specificity of the antibody by staining CB_1R by immunoblot method using neocortex membrane preparation from CB_1R WT and KO mice brain. This antibody recognized major band corresponding to 60 kDa (Tsou et al., 1998; Bisogno et al., 2003) protein and was found in CB_1R WT but absent in CB_1R KO mice brain (Fig. 4*A*). To further assess the contribution of CB_1Rs to the action of ethanol on the developing brain, we determined the CB_1R protein levels by Western blot analysis using a CB_1R-

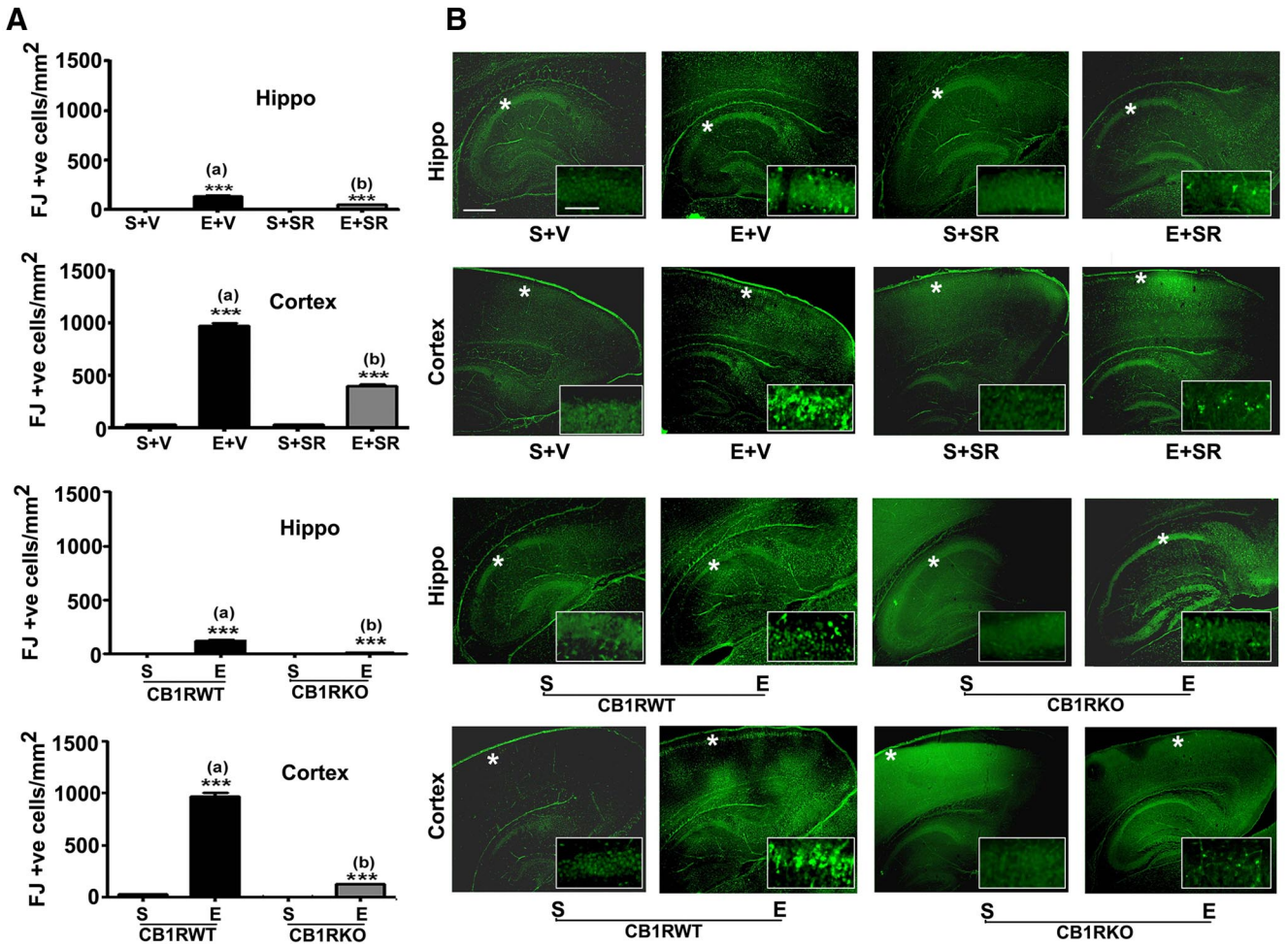

Figure 8. Pharmacological inhibition or genetic deletion of CB_1Rs provides protection against ethanol-induced neurodegeneration in the neonatal mouse brain. ***A***, ***B***, Mice were perfusion fixed 18 h after treatment, and the brain sections from the four treatment groups [saline + vehicle (S+V), ethanol + vehicle (E+V), saline + SR (S+SR), and ethanol + SR (E+SR)] and the CB_1R WT and KO with and without P7 ethanol were stained with F-J. F-J-positive cells were counted in the hippocampus and the retrosplenial cortex (***$p < 0.001$). Two- and one-way ANOVA with Bonferroni's *post hoc* tests were used for statistical analysis (in the one-way ANOVA, the comparison was performed between the S+V vs E+V and E+V vs E+SR). Error bars indicate SEM. (a), Compared with respective saline control; (b), compared with respective ethanol group in all the bar graphs. ***B***, The representative images show the hippocampus and retrosplenial cortex areas. Inset, Higher-magnification photographs showing the F-J-positive neurons (*). Scale bars: 200 μm; insets, 50 μm.

specific antibody. P7 ethanol treatment significantly enhanced CB_1R protein levels in the hippocampus ($F_{(3,28)} = 61, p < 0.001$) and neocortex ($F_{(3,28)} = 26, p < 0.001$) (Fig. 4*B*) at 8 and 24 h time points. This CB_1R protein elevation was accompanied by significantly enhanced mRNA levels in the hippocampus ($F_{(3,28)} = 7, p < 0.01$) and neocortex ($F_{(3,28)} = 5, p < 0.05$) (Fig. 4*C*). These observations suggest that ethanol treatment during the synaptogenic period enhances the expression of CB_1R proteins through the transcriptional activation of the CB_1R gene in the hippocampus and neocortex of the developing brain.

Phosphorylation of ERK1/2 was inhibited after ethanol exposure in neonatal mice

To further assess the contribution of intracellular signaling events to the action of ethanol on the developing brain, we determined the levels of pERK1/2 protein by Western blot analysis using specific phospho-protein antibodies. P7 ethanol treatment significantly reduced the pERK1/2 but not total ERK1/2 protein levels in the hippocampus ($F_{(3,28)} = 16, p < 0.001$) and neocortex ($F_{(3,28)} = 35, p < 0.001$) (Fig. 5) at all the time points measured.

SR prevents and CB_1R KO provides protection against ethanol-induced neurodegeneration

To further evaluate the involvement of CB_1R activity in ethanol-induced neurodegeneration, we used a specific CB_1R antagonist (SR) or CB_1R KO mice and evaluated their ability to prevent the ethanol-induced CB_1R-mediated signaling events and neurodegeneration. In our initial experiments, we assessed whether SR or the deletion of the CB_1Rs would alter ethanol metabolism. The administration of higher dose of SR (1 mg/kg) 30 min before the ethanol treatment did not alter the BALs (BAL peaked at 3 h at 0.48 ± 0.32 g/dl and was gradually reduced to 0.29 ± 0.1 g/dl at 9 h). In addition, the CB_1R KO did not display altered BALs (BAL peaked at 3 h at 0.5 ± 0.29 g/dl and was gradually reduced to 0.27 ± 0.11 g/dl at 9 h). These results together indicate that neither SR treatment nor genetic deletion of the CB_1Rs modulated ethanol metabolism.

We determined the effects of various doses of SR (0.25, 0.5, and 1 mg/kg) on ethanol-induced activation of caspase-3. Our results suggest that SR dose dependently inhibited ethanol-induced activation of caspase-3 (CC3 levels) (Fig. 6*A*). Thus, we used SR at 1 mg/kg in all our subsequent studies. We used several

approaches in our studies after P7 mice treated with saline or ethanol with or without SR. In our first approach, we analyzed the extent of neurodegeneration using several methods. First, we determined the CC3 levels at 8 h by immunohistochemical methods. These results strongly demonstrated that SR significantly prevented caspase-3 activation (reduced CC3 immunostaining) in the hippocampus and cortex brain regions (hippocampus, $F_{(3,33)} = 85$, $p < 0.001$; cortex, $F_{(3,33)} = 745$, $p < 0.001$, two-way ANOVA) (Fig. 6*B*). Two-way ANOVA demonstrated the significant effects of ethanol (vs saline) and a significant interaction between ethanol and SR treatment. Saline and SR–saline groups were not significantly different ($p > 0.05$), whereas ethanol mice had significantly greater proportions of neuronal death in both the retrosplenial cortex and the hippocampus (treatment × CC3-positive cells/mm^2) ($p < 0.001$) (Fig. 6*C*). Analysis of CC3 in the saline- and ethanol-treated P7 CB_1R WT and KO mice suggested that the CB_1R KO compared with the WT mice provided complete protection against P7 ethanol-induced CC3 generation in the hippocampus and cortex (Fig. 6*B*) (hippocampus, $F_{(3,33)} = 70$, $p < 0.001$; cortex, $F_{(3,33)} = 656$, $p < 0.001$, two-way ANOVA) brain regions (Fig. 6*C*), which was consistent with the SR results.

Second, we evaluated CC3 and cTau in the cytosolic extracts of saline- and ethanol-treated hippocampal and neocortical samples by Western blot as additional markers for neurodegeneration. Our results strongly demonstrated that SR pretreatment completely rescued ethanol-induced CC3 and cTau generation in the hippocampus and neocortex ($p < 0.001$) (Fig. 7*A*). A two-way ANOVA with Bonferroni's *post hoc* tests demonstrated the significant effects of ethanol (vs saline) (hippocampus: CC3, $F_{(1,20)} = 175$, $p < 0.001$; cTau, $F_{(1,20)} = 31$, $p < 0.001$; neocortex: CC3, $F_{(1,20)} = 133$, $p < 0.001$; cTau, $F_{(1,20)} = 30$, $p < 0.001$) and SR (vs saline) (hippocampus: CC3, $F_{(1,20)} = 89$, $p < 0.001$; cTau, $F_{(1,20)} = 120$, $p < 0.001$; neocortex: CC3, $F_{(1,20)} = 125$, $p < 0.001$; cTau, $F_{(1,20)} = 92$, $p < 0.001$) and a significant interaction between ethanol and SR (hippocampus: CC3, $F_{(1,20)} = 85$, $p < 0.001$; cTau, $F_{(1,20)} = 49$, $p < 0.001$; neocortex: CC3, $F_{(1,20)} = 133$, $p < 0.001$; cTau, $F_{(1,20)} = 30$, $p < 0.001$). Neither SR nor vehicle alone had any significant effects on CC3 levels in the absence of subsequent ethanol treatment ($p > 0.05$). However, SR significantly reduced cTau levels in saline-treated mice ($p < 0.05$). A comparison with a one-way ANOVA with Bonferroni's *post hoc* tests of CC3 and cTau in saline- and

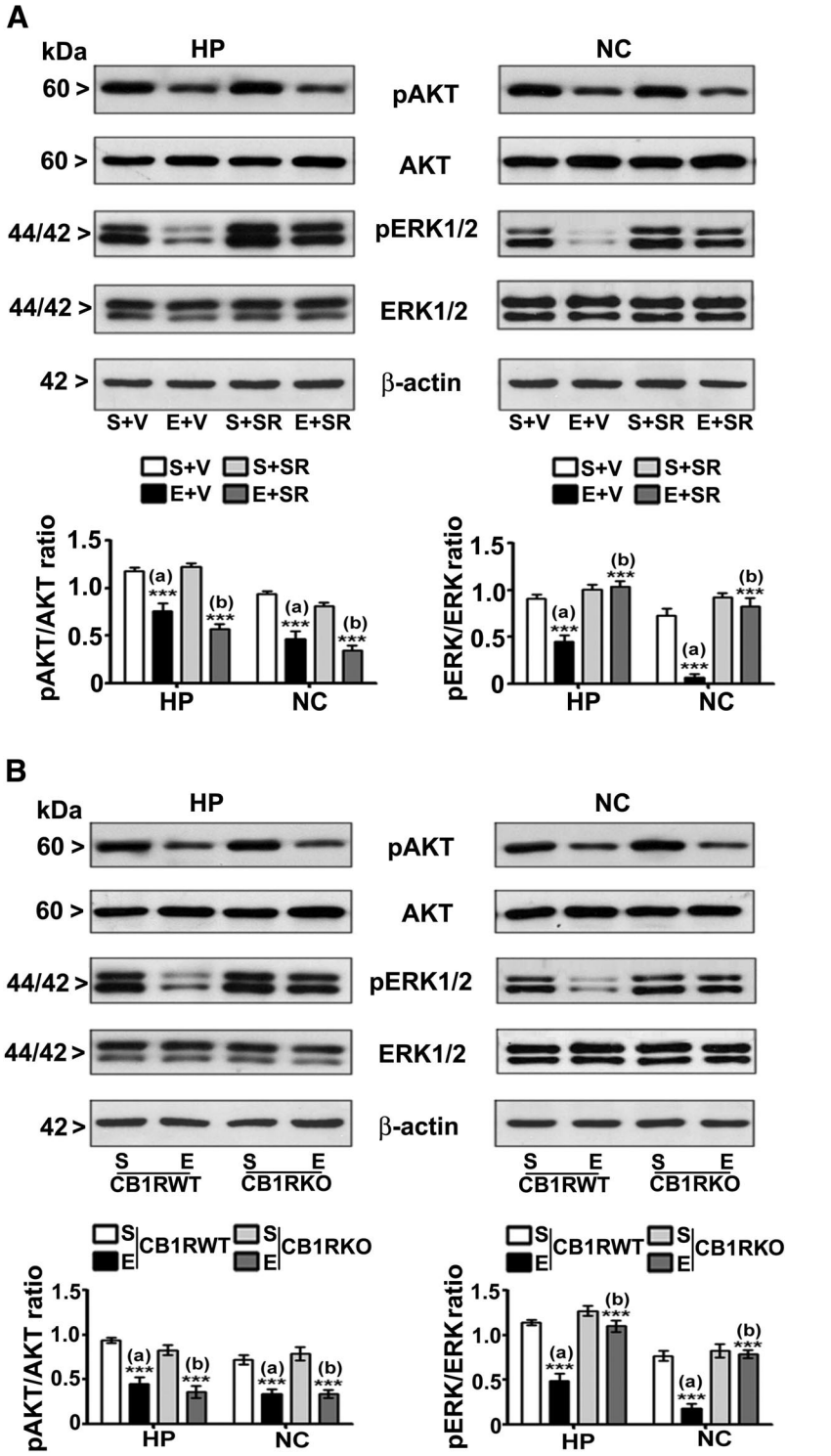

Figure 9. Pharmacological inhibition or genetic deletion of CB_1Rs provides protection against ethanol-induced inhibition of ERK1/2 but not AKT phosphorylation in the neonatal mouse brain. ***A***, Hippocampal and cortical cytosolic extracts from the four treatment groups [saline + vehicle (S+V), ethanol + vehicle (E+V), saline + SR (S+SR), and ethanol + SR (E+SR)] were collected and processed for Western blot to analyze the levels of pERK1/2, ERK1/2, pAKT, and AKT ($n =$ 15 pups per group) (***$p < 0.001$). ***B***, Additional Western blot analyses were performed to determine the levels of pERK1/2, ERK1/2, pAKT, and AKT in the hippocampal and cortical cytosolic extracts obtained from the saline- and ethanol-treated CB_1R WT and KO P7 mice. The representative blots are shown for the hippocampal and cortical cytosolic extracts ($n = 15$ pups per group) (***$p < 0.001$). Two-way ANOVA with Bonferroni's *post hoc* tests was used for statistical analysis. The error bars represent the SEM. (a), Compared with respective saline control; (b), compared with respective ethanol group in all the bar graphs. HP, Hippocampus; NC, neocortex.

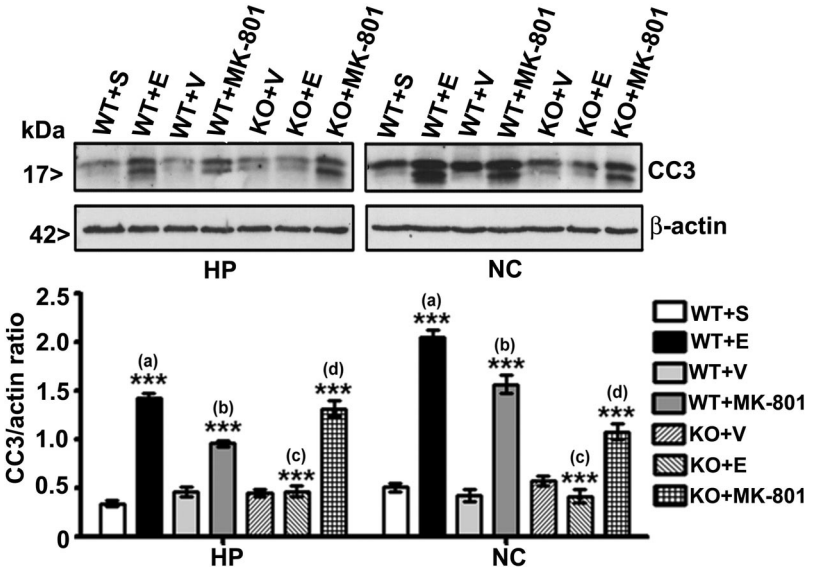

Figure 10. NMDA receptor antagonist induces apoptosis in CB_1R KO mice that are not vulnerable to ethanol-induced apoptosis in P7 mice. Hippocampal and cortical cytosolic extracts from the various treatment groups [WT + saline (WT+S), WT + ethanol (WT+E), WT + vehicle (WT+V), WT + MK-801, KO + vehicle (KO+V), KO + ethanol (KO+E), and KO + MK-801] were collected and processed for Western blot to analyze the levels of CC3 ($n = 10$ pups per group) (***$p < 0.001$). One-way ANOVA with Bonferroni's *post hoc* tests was used for statistical analysis. The error bars represent the SEM. (a), compared with respective saline control; (b), compared with respective ethanol group; (c), compared to respective WT ethanol group; (d), compared to KO vehicle group in all the bar graphs. HP, Hippocampus; NC, neocortex.

ethanol-treated P7 CB_1R WT and KO mice suggested that, consistent with the SR treatment, the CB_1R KO compared with the WT mice provided protection against P7 ethanol-induced neurodegeneration in the hippocampus (CC3, $F_{(3,20)} = 260, p < 0.001$; cTau, $F_{(3,20)} = 67, p < 0.001$) and neocortex (CC3, $F_{(3,20)} = 104, p < 0.001$; cTau, $F_{(3,20)} = 64, p < 0.001$) (Fig. 7*B*). CB_1R KO mice treated with saline showed significantly reduced cTau ($p < 0.05$) and normal CC3 levels as observed for SR alone.

In our third approach, the extent of the neurodegeneration was evaluated by F-J staining (Wilson et al., 2011; Sadrian et al., 2012). The results of the F-J staining demonstrated that SR significantly reduced the number of F-J-positive cells in the SR–ethanol groups (compared with the ethanol group) in the hippocampus ($F_{(3,36)} = 535$, $p < 0.001$) and cortex ($F_{(3,12)} = 1024$, $p < 0.001$, two-way ANOVA) (Fig. 8*A*). Analysis of the F-J staining in the saline- and ethanol-treated P7 CB_1R WT and KO mice suggested that P7 CB_1R KO mice provided protection against ethanol-induced neurodegeneration in the hippocampus ($F_{(3,45)} = 828$, $p < 0.001$) and cortex ($F_{(3,45)} = 776$, $p < 0.001$, one-way ANOVA) (Fig. 8*A*) brain regions. Representative images used for the F-J quantitative analysis are provided in Figure 8*B*. Together, these data indicated that the ethanol-induced activation of CB_1R function contributes to neurodegeneration in the developing brain.

Neuroprotective effects of CB_1R blockade involves pERK1/2 but not the phosphatidylinositol 3/AKT pathway

To elucidate the downstream intracellular pathways involved in the protective effects of the CB_1R blockade, we studied the involvement of the phosphatidylinositol 3 kinase (PI3K)/AKT pathway, a key regulator of cell survival (Luikart et al., 2008). Although a previous study had shown that AKT phosphorylation was reduced at 8 h after ethanol treatment in P7 mice (Chakraborty et al., 2008), it is not clear whether AKT pathway deficits are responsible for ethanol-induced neurodegeneration. We investigated whether pretreatment of SR, which prevents ethanol-induced neurodegeneration, could rescue these ethanol-induced pAKT deficits. Our results suggest that AKT phosphorylation was not rescued by SR pretreatment (compared with the ethanol group) in the hippocampus ($F_{(3,20)} = 3$, $p > 0.05$) and neocortex ($F_{(3,20)} = 1.3, p > 0.05$, two-way ANOVA) (Fig. 9*A*). We assessed the total amount of AKT proteins. We found that the total AKT protein levels were not altered in the ethanol-treated samples compared with the saline samples. In addition, SR did not alter the AKT protein levels in either the ethanol or saline samples (Fig. 9*A*). Similarly, CB_1R KO mice, which lack ethanol-induced neurodegeneration, did not provide protection against P7 ethanol-induced inhibition of AKT phosphorylation in the hippocampus ($F_{(3,20)} = 22$, $p < 0.001$) and neocortex ($F_{(3,20)} = 18$, $p < 0.001$, one-way ANOVA) (Fig. 9*B*). Together, these findings not only imply that ethanol-induced inhibition of pAKT are not mediated by CB_1R activation but also suggest that pAKT deficits may not be necessary for ethanol-induced neurodegeneration. Thus, we investigated the involvement of other pathways, such as the MAPK signaling pathway, which had been reported previously to mediate cell survival (Grossmann, 2002). Notably, P7 ethanol treatment has been shown to inhibit this pathway (Fig. 5) (Young et al., 2008).

We evaluated the phosphorylation state of ERK1/2 using a phospho-specific antibody. The phosphorylation of ERK1/2 was decreased in P7 ethanol-treated hippocampal and neocortex tissues compared with saline-treated samples (Fig. 5). Furthermore, pharmacological blockade of CB_1Rs before P7 ethanol treatment significantly rescued the ethanol-induced inhibition of pERK1/2 levels in both the hippocampus and neocortex. A two-way ANOVA with Bonferroni's *post hoc* tests demonstrated the significant effects of ethanol (vs saline) (hippocampus: $F_{(1,20)} = 15, p < 0.001$; neocortex: $F_{(1,20)} = 33$, $p < 0.001$) and SR (vs saline) (hippocampus: $F_{(1,20)} = 38$, $p < 0.001$; neocortex: $F_{(1,20)} = 53$, $p < 0.001$) and a significant interaction between ethanol and SR (hippocampus: $F_{(1,20)} = 19$, $p < 0.001$; neocortex: $F_{(1,20)} = 19$, $p < 0.001$). Neither SR nor vehicle alone had any significant effects on the pERK1/2 levels in the absence of subsequent ethanol treatment ($p > 0.05$) (Fig. 9*A*). An analysis of the pERK1/2 levels in the saline- and ethanol-treated P7 CB_1R WT and KO mice suggested that the CB_1R KO mice compared with WT were protected against P7 ethanol-induced inhibition of pERK1/2 protein levels in the hippocampus ($F_{(3,20)} = 33$, $p < 0.001$) and neocortex ($F_{(3,20)} = 29$, $p < 0.001$, one-way ANOVA) (Fig. 9*B*). These results suggest that the ERK1/2 pathway is involved in neuronal survival downstream of the CB_1Rs in the developing brain and is compromised by ethanol treatment. These observations together strongly suggest that P7 ethanol-induced neurodegeneration is mediated by the CB_1R–MAPK cascade but not by the PI3K/AKT pathway in the developing brain.

Previous studies have shown that apoptotic effects of ethanol were attributed to its antagonist effects at NMDA receptors (Ikonomidou et al., 2000b). In our CB_1R KO studies, ethanol failed to induce apoptosis (Figs. 6, 7*B*, 8), suggesting that CB_1R

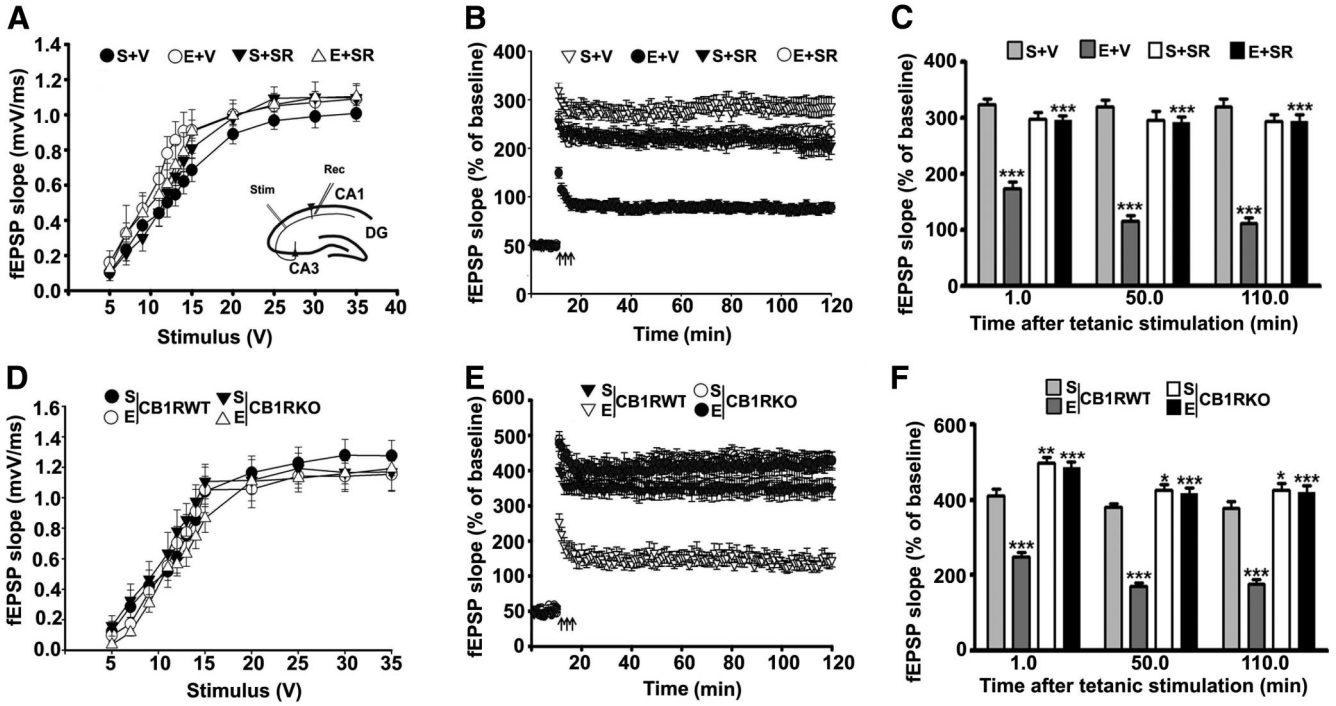

Figure 11. Pharmacological inhibition or genetic deletion of CB_1R activity before ethanol treatment during brain development prevents long-lasting synaptic deficits in the adult mice. ***A***, A summary graph showing the field I/O relationships for P7 saline + vehicle (S+V), ethanol + vehicle (E+V), saline + SR (S+SR), and ethanol + SR (E+ SR). Inset, A schematic diagram showing the stimulating and recording electrode positions in the CA1 region of the hippocampus. ***B***, A time course of the averages of the fEPSP slopes from the slices obtained from the S+V-, E+V-, S+SR-, and E+SR-treated mice. The fEPSP slopes were normalized to the average value during the 10 min before stimulation in each experiment. The arrows show the time of tetanic stimulation (4 pulses at 100 Hz, with bursts repeated at 5 Hz, and each tetanus including 3 10-burst trains separated by 15 s). ***C***, A combined plot of the averages of fEPSP slopes at several time points. ***D***, Additional experiments analyzed the I/O relationship in P7 saline- and ethanol-treated CB_1R WT and KO mice. ***E***, A time course of the fEPSP slopes from the slices derived from P7 saline- and ethanol-treated CB_1R WT and KO mice. ***F***, A combined plot of the averages of the fEPSP slopes at several time points for P7 saline- and ethanol-treated CB1 WT and KO mice. Each point is the mean ± SEM ($n = 5$ mice per group, 10 slices per group). Two-way ANOVA with Bonferroni's *post hoc* test; $^{***}p < 0.001$.

acts as an intermediate molecule in the apoptotic action of ethanol through NMDA receptors. To understand whether directly blocking NMDA receptors in CB_1R KO mice induces apoptosis, we treated P7 CB_1R WT and KO mice with NMDA receptor antagonist (MK-801) for 24 h. We determined the levels of CC3 protein by Western blot analysis. MK-801 treatment significantly increased CC3 levels (Ikonomidou et al., 2000b) in the hippocampus ($p < 0.001$) and neocortex ($p < 0.001$) in both CB_1R WT and KO mice (Fig. 10) compared with vehicle or saline treatment. These findings suggest that, although CB_1R KO mice, like WT mice, have the ability to induce apoptosis through NMDA receptor blockade, they failed to induce apoptosis by ethanol treatment (Figs. 6*B*,*C*, 7*B*, 8, 10). These observations collectively suggest that activation of CB_1R negatively regulates NMDA receptor function (Basavarajappa et al., 2008), followed by apoptosis in the developing brain.

The pharmacological inhibition or genetic ablation of CB_1Rs before ethanol treatment in P7 mice prevents ethanol-induced synaptic plasticity and memory deficits in adult mice

Ethanol treatment during early brain development causes deficits in synaptic function (Vaglenova et al., 2008) that persist into adulthood (Wilson et al., 2011; Sadrian et al., 2012). The molecular mechanisms responsible for these long-lasting deficits are essentially unknown. First, we performed *in vitro* adult hippocampal slice recordings to examine whether CB_1R blockade, which protects neurons from P7 ethanol-induced deficits in pERK1/2 and neurodegeneration, rescues ethanol-induced long-lasting impairments in synaptic plasticity. We determined the input/output (I/O) responses of fEPSP and LTP of fEPSP in the Schaffer collateral pathway of the hippocampal slices (Fig. 11*A*, inset) prepared from adult animals treated with saline, ethanol, SR, and ethanol + SR at P7. Increasing stimulus intensity evoked robust I/O responses of fEPSP in all of the groups. The I/O curve of fEPSP was not altered by ethanol, SR, or ethanol + SR treatment ($p > 0.05$) (Fig. 11*A*). These findings suggest that neither ethanol nor SR significantly affects the magnitude of fEPSP in pyramidal cells over the entire range of stimulation intensities. Before tetanic stimulations, the baseline fEPSP was recorded in 60 s intervals with stimulation at an intensity equivalent to ~35% of the maximum evoked response. The tetanic stimulation evoked a typical LTP of fEPSP (Vitolo et al., 2002; Sadrian et al., 2012) (Fig. 11*B*) in slices from adult mice treated at P7 with saline + vehicle, ethanol + vehicle, SR, or ethanol + SR. These responses were stable over 120 min. However, tetanic stimulation evoked a significantly reduced LTP magnitude of fEPSP in slices ($n = 10$ slices/5 mice/group) prepared from the P7 ethanol-treated animals (1 min, 227 ± 11; 50 min, 177 ± 10; and 110 min, 173 ± 10) compared with slices from the saline-treated animals (1 min, 344 ± 11; 50 min, 314 ± 12; and 110 min, 314 ± 13) ($p < 0.001$) with a significant group interaction [two-way ANOVA (saline-vehicle group, ethanol group × saline–vehicle group, SR treatment): $F_{(1,44)} = 50$, $p < 0.001$; *post hoc* test: saline vs ethanol were significantly different at all posttetanic stimulation time intervals (1, 50, and 110 min), $p < 0.001$]. The magnitude of the LTP of fEPSP in the slices prepared from the SR-treated animals (1 min, 339 ± 11; 50 min, 307 ± 16; 110 min, 315 ± 11) did not differ significantly from that observed in the slices from saline-

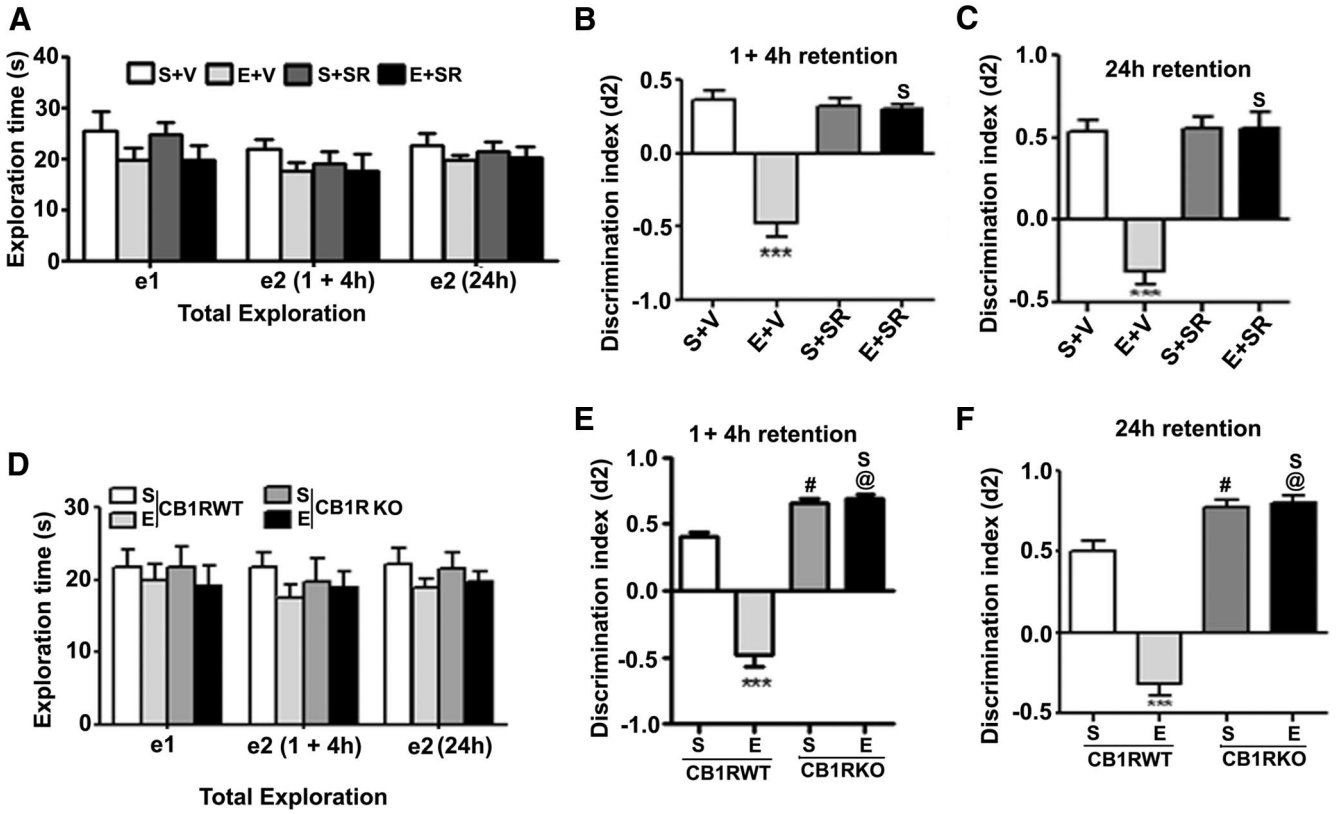

Figure 12. Inactivation of CB_1R activity before ethanol treatment during brain development prevents ORM loss in adult mice. ***A***, Level of exploration was measured at el, e2 (1 + 4 h), and e2 (24 h), and the time spent in exploring the two objects in T1 and T2 (at 1 + 4 and 24 h) by saline + vehicle (S+V)-treated, ethanol + vehicle (E+V)-treated, saline + SR (S+SR)-treated, and ethanol + SR (E+SR)-treated mice. ***B***, Discrimination indices (d2) obtained from the S+V-, E+V-, S+SR-, and E+ SR-treated mice at 1 and 4 h (combined) retention intervals. ***C***, Discrimination indices (d2) obtained from the S+V-, E+V-, S+SR-, and E+ SR-treated mice at 24 h retention intervals. $^{***}p < 0.001$ versus S+V; $^{\$}p < 0.001$ versus E+V. ***D***, Level of exploration was measured at el, e2 (1 + 4 h), and e2 (24 h) and the time spent in exploring the two objects in T1 and T2 (at 1 + 4 and 24 h) by P7 saline- and ethanol-treated CB_1R WT and KO mice. ***E***, Discrimination indices (d2) obtained from the P7 saline- and ethanol-treated CB_1R WT and KO mice at 1 and 4 h (combined) retention intervals. ***F***, Discrimination indices (d2) obtained from the P7 saline- and ethanol-treated CB_1R WT and KO mice at 24 h retention intervals. Each point is the mean ± SEM ($n = 8$ mice per group). One-way ANOVA with Bonferroni's *post hoc* test; $^{***}p < 0.001$ versus S+CB1WT; $^{\#}p < 0.05$ versus S+CB1WT; $^{\$}p < 0.05$ versus S+CB1WT; $^{@}p < 0.001$ versus E+CB1WT.

treated mice ($p > 0.05$). The SR pretreatment completely rescued the P7 ethanol-induced defects in the LTP magnitude of fEPSP, for both the initial induction and maintenance, extending over a 120 min period [1 min, 300 ± 9; 50 min, 271 ± 11; 110 min, 273 ± 14; *post hoc* test: ethanol vs ethanol + SR significantly different at all posttetanic stimulation time intervals (1, 50, and 110 min); $p < 0.001$] (Fig. 11*C*).

We then examined whether CB_1R KO mice were protected against P7 ethanol-induced deficits in synaptic plasticity. Our results suggest that CB_1R WT and KO mice exhibited similar robust I/O responses of fEPSP evoked by increasing stimulus intensity. The I/O curve of fEPSP was not altered by ethanol in the WT and KO mice ($p > 0.05$) (Fig. 11*D*). These findings suggest that neither ethanol nor genetic deletion of CB_1Rs significantly affects the magnitude of fEPSP in pyramidal cells over the entire range of stimulation intensities. Tetanic stimulation evoked a typical LTP of fEPSP (Puzzo et al., 2009; Sadrian et al., 2012) (Fig. 11*E*) in slices from adult WT mice treated at P7 with saline or ethanol. These responses were stable over 120 min. However, tetanic stimulation evoked a significantly reduced LTP magnitude of fEPSP in slices ($n = 10$ slices/5 mice/group) prepared from P7 ethanol-treated WT animals (1 min, 249 ± 11; 50 min, 173 ± 8; and 110 min, 178 ± 10) compared with saline-treated WT animals (1 min, 359 ± 17; 50 min, 320 ± 11; and 110 min, 332 ± 17) ($p < 0.001$). The magnitude of LTP of fEPSP in slices prepared from ethanol-treated CB_1R KO animals (1 min, 355 ± 16; 50 min, 326 ± 14; and 110 min, 305 ± 13) differed significantly from that in slices from the saline-treated KO mice (1 min, 419 ± 16; 50 min, 376 ± 15; and 110 min, 386 ± 17) ($p > 0.05$). The genetic deletion of the CB_1Rs provided complete protection against P7 ethanol-induced defects in the LTP magnitude of fEPSP, for both the initial induction and maintenance, and extended over a 120 min period [*post hoc* test: CB_1R KO–saline vs CB_1R KO–ethanol were not significantly different at any posttetanic stimulation time intervals (1, 50, 110 min); $p > 0.05$] (Fig. 11*F*). However, CB_1R KO mice exhibited an enhanced LTP magnitude compared with WT or regular C57BL/6J saline-treated mice (1 min: $F_{(3,36)} = 22$, $p < 0.001$; 50 min: $F_{(3,36)} = 44$, $p < 0.001$; 110 min: $F_{(3,36)} = 30$, $p < 0.001$; one-way ANOVA).

Next we investigated the ORM to examine whether CB_1R blockade rescues ethanol-induced memory impairments. Results indicate that P7 ethanol or SR treatment has no significant effects on exploration times (e1 or e2) in the ORM task [e1, $F_{(3,28)} = 1.0$, $p > 0.05$; e2 (1 + 4 h), $F_{(3,28)} = 1.2$, $p > 0.05$; e2 (24 h), $F_{(3,28)} = 1.5$, $p > 0.05$; one-way ANOVA] (Fig. 12*A*). Ethanol treatment at P7 impaired ORM performance both at 1 and 4 h retention (short-term memory) and was rescued in mice treated with SR ($F_{(3,60)} = 43$, $p < 0.001$; one-way ANOVA) (Fig. 12*B*) before P7 ethanol administration as observed with LTP. Because the discrimination index (d2) was similar between 1 and 4 h retention time, we have combined these data for clarity. Ethanol treatment at P7 also impaired long-term ORM performance at 24 h reten-

tion (long-term memory) and was rescued in mice treated with SR ($F_{(3,20)} = 35$, $p < 0.001$; one-way ANOVA) (Fig. 12*C*) before P7 ethanol administration. We then examined whether CB_1R KO mice were protected against P7 ethanol-induced deficits in ORM performance. P7 ethanol administration has no significant effects on adult CB_1R WT or KO mice exploration times (e1 or e2) in the ORM task [e1, $F_{(3,28)} = 0.28$, $p > 0.05$; e2 (1 + 4 h), $F_{(3,28)} = 0.5$, $p > 0.05$; e2 (24 h), $F_{(3,28)} = 0.4$, $p > 0.05$; one-way ANOVA) (Fig. 12*D*). Ethanol treatment at P7 also impaired both short-term ($F_{(3,60)} = 91$, $p < 0.001$; one-way ANOVA) and long-term ($F_{(3,20)} = 41$, $p < 0.001$; one-way ANOVA) ORM performance in CB_1R WT mice. The magnitude of short-term (Fig. 12*E*) and long-term (Fig. 12*F*) ORM performance was enhanced in CB_1R KO mice compared with WT mice ($p < 0.001$) as observed in a previous study (Reibaud et al., 1999). Furthermore, CB_1R KO mice provided protection against P7 ethanol-induced deficits at both short-term and long-term ORM performance (*post hoc* test: CB_1R KO–saline vs CB_1R KO–ethanol were not significantly different, $p > 0.05$) as observed with our LTP data. Together, these findings are consistent with previous studies that demonstrate enhanced hippocampal LTP and ORM task (Reibaud et al., 1999; Bohme et al., 2000) in CB_1R KO compared with WT mice. Therefore, blocking CB_1R function before P7 ethanol exposure prevents synaptic and memory deficits in adult mice (Fig. 13).

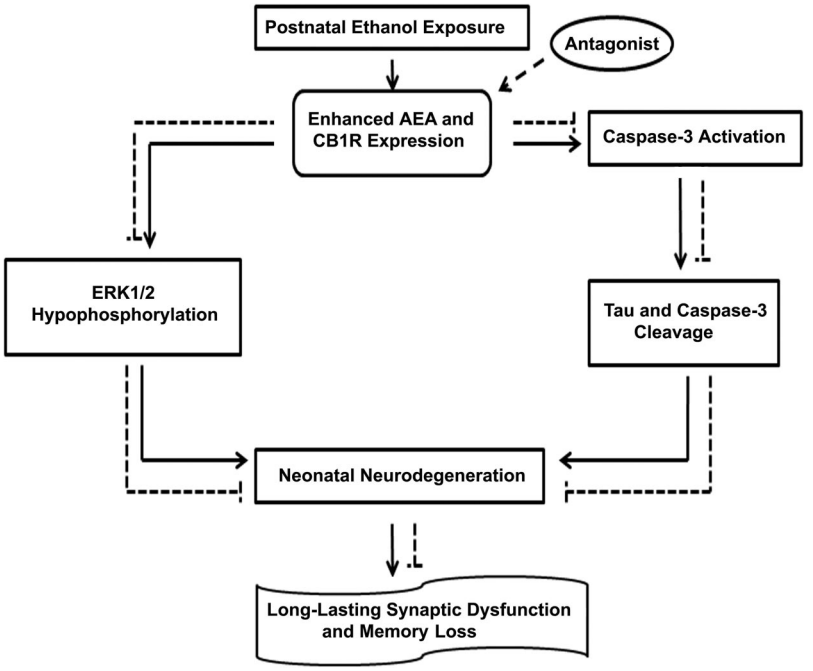

Figure 13. A schematic representation of the proposed mechanism of action by which AEA/CB_1R/ERK1/2 signaling regulates ethanol-induced neurodegeneration, leading to neurobehavioral deficits in adult mice. P7 ethanol enhances AEA/CB_1Rs (AEA tone), which causes ERK1/2 hypophosphorylation, caspase-3 activation, and tau cleavage, and leads to neonatal neurodegeneration (⟶). In previous studies, CB_1R activation was shown to inhibit NMDA receptor function in several experimental models (Twitchell et al., 1997; Hampson et al., 2011), and ethanol was shown to inhibit glutamatergic neurotransmission via CB_1R activation (Basavarajappa et al., 2008). These events during postnatal development may disrupt the refinement of neuronal circuits (Wilson et al., 2011; Sadrian et al., 2012) and lead to long-lasting deficits in synaptic plasticity and memory in adult animals. The inhibition of CB_1Rs (dotted lines) (AEA tone) prevents pERK1/2 hypophosphorylation and neonatal neurodegeneration (Tau and caspase-3 cleavage), which results in normal neurobehavioral function in adult mice. The genetic ablation of CB_1Rs does not affect the NMDA receptor antagonist-induced apoptosis but provides protection against ethanol-induced neonatal neurodegeneration and synaptic and memory deficits in adult mice. Therefore, the putative AEA/CB_1R/pERK1/2 signaling mechanism may have a potential regulatory role in neuronal function in the developing brain and may be a valuable therapeutic target for FASD.

Discussion

There is a growing interest in the role of ECs and their CB_1Rs in the regulation of neuronal migration, axonal elongation, and synaptogenesis during early brain development (Morozov and Freund, 2003; Mulder et al., 2008). In this study, we demonstrate for the first time that single-day ethanol treatment at P7 enhances the EC "tone" (increased AEA synthesis and/or CB_1R abundance) within the hippocampal and cortical brain regions and contributes to the neurodegeneration in the developing brain and persistent synaptic and memory deficits in adult mice (Fig. 13). Indeed, the detrimental effects of ethanol were counteracted by the CB_1R antagonist SR, suggesting that the actions of ethanol are mediated via enhanced AEA biosynthesis and the subsequent activation of CB_1Rs rather than via altered ethanol metabolism by the SR. In addition, a previous study has demonstrated that SR does not affect the alcohol metabolism (Colombo et al., 1998). Furthermore, our study revealed that neonatal CB_1R KO mice were less susceptible to ethanol-induced neurodegeneration compared with WT mice. This effect cannot be explained by an altered metabolism of ethanol in the CB_1R KO mice, because these neonatal mice have similar BALs to WT mice after receiving the same ethanol concentration. In several cases, the CB_1R KO adult mice have similar (Wang et al., 2003) or higher (Lallemand and de Witte, 2005) BALs than WT mice after receiving the same concentration of ethanol.

In addition, we found that ethanol-induced increase in AEA levels may be attributable to either enhanced synthesis (Basavarajappa and Hungund, 1999; Basavarajappa, 2007a) via its precursor NAPE (Basavarajappa and Hungund, 1999; Chakraborty et al., 2008) and glycerophospho-*N*-arachidonoylethanolamine (GDE1). Because there was no alteration of FAAH (Di Marzo et al., 1994; Cravatt et al., 1996; Basavarajappa et al., 2006) protein levels by ethanol and our experimental data indicated enhanced NAPE–PLD and GDE1 protein levels through the transcriptional activation of the NAPE–PLD and GDE1 gene, respectively, we propose that the P7 ethanol-induced increase in AEA levels in the developing brain may be attributable to enhanced NAPE–PLD and GDE1 activity, a major source for the release of acylethanolamides (Giuffrida et al., 1999; Basavarajappa, 2007b). Additional pathways have been suggested to play an important role in the formation of AEA in NAPE–PLD and GDE1 KO mice via multistep reactions (Simon and Cravatt, 2010), and additional studies are needed to clarify whether ethanol in the developing brain may also activate these additional pathways to generate AEA. It is also possible that lack of net increase in 2-AG levels may be attributable to differential effects of P7 ethanol on 2-AG synthesis (diacylglycerol lipases) or degradation (monoacylglycerol lipase). Therefore, we are currently investigating this possibility. Nevertheless, enhanced AEA activity may lead to abnormal development of synaptic connection (for review, see Basavarajappa et al., 2009) during early brain development

and may partially explain the neurobehavioral disturbances associated with FASD.

Various studies support the notion that ECs play a critical role via CB_1Rs in the control of neuronal fate (Morozov and Freund, 2003; Mulder et al., 2008). In addition to enhanced AEA levels, we also found significant increase in CB_1R expression in hippocampal and cortical brain in which ethanol induces neonatal neurodegeneration. Interestingly, the prevailing *in vitro* effects of CB_1R activation in young cultured neurons are the inhibition of dendritogenesis, dendritic outgrowth, and, to a lesser extent, axonal outgrowth, with the latter effect being more pronounced at later developmental stages (Vitalis et al., 2008). These data, together with our findings showing that CB_1R KO mice, which have the ability to exhibit apoptosis by NMDA receptor blockade, are not susceptible to ethanol-induced neonatal neurodegeneration and that the CB_1R antagonist SR prevents neurodegeneration induced by ethanol, support a critical role of CB_1R in neuronal survival and function during early brain development. Importantly, the lack of marked brain developmental deficits in various KO mice, which are deficient for different components of the EC system, including CB_1Rs, is attributable to the existence of powerful compensatory mechanisms and high functional plasticity (Harkany et al., 2008) in the developing brain. Taken as a whole, the overall regulatory role in the neurodegeneration suggests that postnatal CB_1R signaling is one of key players that help to establish proper neuronal connectivity, which is compromised in the ethanol-exposed offspring and may be responsible for the neuronal dysfunction and memory loss observed in this model as well as other animal models of FASD (Petkov et al., 1991; Vaglenova et al., 2008; Wilson et al., 2011; Sadrian et al., 2012). It should be noted that AEA not only activates CB_1R but also other receptors, such as transient receptor potential vanilloid 1 (Starowicz et al., 2007) and CB_2 (Mechoulam and Parker, 2013) in the brain. Activation of these receptors by AEA may also contribute to the observed neurodegeneration in the brain. However, such possibility may not exist in the developing brain because P7 ethanol failed to induce neurodegeneration in CB_1R KO mice.

It has been shown that the ERK1/2 and PI3K/AKT (PKB) pathways work in a coordinate or synergistic manner (Worster et al., 2012) and have been implicated in essential aspects of neuronal survival and axonal and dendritic morphogenesis during nervous system development (Huang and Reichardt, 2001; Luikart et al., 2008). Consistent with previous reports, our findings point to ERK and the AKT pathway as major intracellular signaling events in the P7 ethanol-induced neonatal neurodegeneration (Young et al., 2008). However, the present study has demonstrated that the ERK pathway is a major downstream target of neuroprotection provided by CB_1R blockade. Interestingly, the AKT pathway apparently did not contribute to the neuroprotection mediated by CB_1R blockade, because neither SR nor genetic deletion of the CB_1Rs counteracted the suppressant effect of ethanol on pAKT. Consistent with our observations, it was shown that the neuroprotective effect of lithium against ethanol-induced neonatal neurodegeneration was mediated by pERK but not by the pAKT pathway (Young et al., 2008). However, AKT suppression alone was ineffective in inducing apoptosis but became markedly effective if the ERK pathway was simultaneously suppressed (Marushige and Marushige, 1999). These observations support the presence of a remarkable specificity involving the AEA/CB_1R/ERK pathway in the regulation of ethanol-induced neonatal neurodegeneration. Moreover, ethanol exposure during the third trimester (P7) produces profound functional and structural alterations in the hippocampus (Livy et al., 2003; Galindo et al., 2005), and our findings suggest that dysregulation of AEA/CB_1R/ERK pathway may significantly contribute to long-term neurobehavioral deficits commonly associated with FASD (Izumi et al., 2005; Medina, 2011; Wilson et al., 2011; Sadrian et al., 2012).

The predominant and immediate effect of EC-mediated CB_1R activation is the decrease in NMDA receptor function (Basavarajappa et al., 2008; Puighermanal et al., 2009) and increase in GABA release (Bernard et al., 2005). Consistent with these observations, our previous double patch-clamp recordings in cultured hippocampal neurons derived from P1 mice suggest that ethanol-induced ECs are responsible for the decrease in hippocampal synaptic plasticity (Basavarajappa et al., 2008). Findings from neonatal rats suggest that ethanol may actually affect CA3 pyramidal neurons via inhibition of the postsynaptic AMPARs, which results in a decrease in glutamatergic release (Mameli et al., 2005). In fact, this study is consistent with the study conducted by Twitchell et al. (1997) in which exogenous cannabinoids inhibit glutamatergic release by activating CB_1R-mediated inhibition of N-type and P/Q-type calcium channels (Twitchell et al., 1997) and may be responsible for the enhanced susceptibility of immature brain to ethanol neurotoxicity (Hansen et al., 2008).

Ethanol exposure importantly affects several neurotransmitter systems (e.g., serotonin and glutamate) (Ikonomidou et al., 2000a, 2001; Zhou et al., 2001, 2005), as well as intercellular and intracellular signaling factors (e.g., Ca^{2+} and cAMP) involved in many aspects of brain development, including in the establishment of neuronal circuits and mental and behavioral abnormalities (Vaglenova et al., 2008; Gil-Mohapel et al., 2010; Medina, 2011). Furthermore, a large number of studies have reported that developmental exposure to exogenous cannabinoids can also affect development of multiple neurotransmitter systems, including catecholaminergic, serotonergic, GABAergic, glutamatergic, and opioid systems (Fernández-Ruiz et al., 2000, 2004; Wang et al., 2006), leading to long-term behavioral deficits (Schneider, 2009). Postnatal exposure to exogenous cannabinoids, although less well investigated, may also result in long-term behavioral deficits (Campolongo et al., 2011). These collective studies suggest that developmental exposures to ethanol or exogenous cannabinoids can impact multiple neurotransmitter systems, and the current study for the first time demonstrates that exposure to ethanol during postnatal period alters the natural levels of the AEA as well as CB_1Rs and limits NMDA receptor function in neonatal mice, causing lasting morphological changes underscoring the synaptic and memory deficits.

A significant aspect of our study is the demonstration of AEA/CB_1R/pERK1/2 signaling as a critical regulator of early neuronal function and its importance in neuronal survival (Fig. 13). Unraveling the unique and complex mechanisms of CB_1R signaling in the developing brain would help better target the pathways responsible for generating cell death and long-lasting neurobehavioral deficits after alcohol exposure in the immature brain and inform the search for novel treatments of FASD.

References

Alexinsky T, Chapoutier G (1978) A new behavioral model for studying delayed response in rats. Behav Biol 24:442–456.

Bacci A, Huguenard JR, Prince DA (2004) Long-lasting self-inhibition of neocortical interneurons mediated by endocannabinoids. Nature 431:312–316. CrossRef Medline

Basavarajappa BS (2007a) Critical enzymes involved in endocannabinoid metabolism. Protein Pept Lett 14:237–246. CrossRef Medline

Basavarajappa BS (2007b) The endocannabinoid signaling system: a potential target for next-generation therapeutics for alcoholism. Mini Rev Med Chem 7:769–779. CrossRef Medline

Basavarajappa BS (2007c) Endocannabinoid signaling and alcohol addiction. In: New research on alcoholism (Baye DR, ed), pp 1–55. New York: Nova Science Publishers.

Basavarajappa BS (2007d) Neuropharmacology of the endocannabinoid signaling system: molecular mechanisms, biological actions and synaptic plasticity. Curr Neuropharmacol 5:81–97. CrossRef Medline

Basavarajappa BS, Hungund BL (1999) Chronic ethanol increases the cannabinoid receptor agonist, anandamide and its precursor N-arachidonyl phosphatidyl ethanolamine in SK-N-SH Cells. J Neurochem 72:522–528. CrossRef Medline

Basavarajappa BS, Hungund BL (2001) Cannabinoid receptor agonist-stimulated [^{35}S]guanosine triphosphateγS binding in the brain of C57BL/6 and DBA/2 mice. J Neurosci Res 64:429–436. CrossRef Medline

Basavarajappa BS, Saito M, Cooper TB, Hungund BL (2003) Chronic ethanol inhibits the anandamide transport and increases extracellular anandamide levels in cerebellar granule neurons. Eur J Pharmacol 466:73–83. CrossRef Medline

Basavarajappa BS, Yalamanchili R, Cravatt BF, Cooper TB, Hungund BL (2006) Increased ethanol consumption and preference and decreased ethanol sensitivity in female FAAH knockout mice. Neuropharmacology 50:834–844. CrossRef Medline

Basavarajappa BS, Ninan I, Arancio O (2008) Acute ethanol suppresses glutamatergic neurotransmission through endocannabinoids in hippocampal neurons. J Neurochem 107:1001–1013. CrossRef Medline

Basavarajappa BS, Nixon RA, Arancio O (2009) Endocannabinoid system: emerging role from neurodevelopment to neurodegeneration. Mini Rev Med Chem 9:448–462. CrossRef Medline

Bayer SA, Altman J, Russo RJ, Zhang X (1993) Timetables of neurogenesis in the human brain based on experimentally determined patterns in the rat. Neurotoxicology 14:83–144. Medline

Berghuis P, Rajnicek AM, Morozov YM, Ross RA, Mulder J, Urbán GM, Monory K, Marsicano G, Matteoli M, Canty A, Irving AJ, Katona I, Yanagawa Y, Rakic P, Lutz B, Mackie K, Harkany T (2007) Hardwiring the brain: endocannabinoids shape neuronal connectivity. Science 316:1212–1216. CrossRef Medline

Bernard C, Milh M, Morozov YM, Ben-Ari Y, Freund TF, Gozlan H (2005) Altering cannabinoid signaling during development disrupts neuronal activity. Proc Natl Acad Sci U S A 102:9388–9393. CrossRef Medline

Bisogno T, Howell F, Williams G, Minassi A, Cascio MG, Ligresti A, Matias I, Schiano-Moriello A, Paul P, Williams EJ, Gangadharan U, Hobbs C, Di Marzo V, Doherty P (2003) Cloning of the first sn1-DAG lipases points to the spatial and temporal regulation of endocannabinoid signaling in the brain. J Cell Biol 163:463–468. CrossRef Medline

Bohme GA, Laville M, Ledent C, Parmentier M, Imperato A (2000) Enhanced long-term potentiation in mice lacking cannabinoid CB1 receptors. Neuroscience 95:5–7. CrossRef Medline

Campolongo P, Trezza V, Ratano P, Palmery M, Cuomo V (2011) Developmental consequences of perinatal cannabis exposure: behavioral and neuroendocrine effects in adult rodents. Psychopharmacology (Berl) 214:5–15. CrossRef Medline

Chakraborty G, Saito M, Mao RF, Wang R, Vadasz C, Saito M (2008) Lithium blocks ethanol-induced modulation of protein kinases in the developing brain. Biochem Biophys Res Commun 367:597–602. CrossRef Medline

Colombo G, Agabio R, F à M, Guano L, Lobina C, Loche A, Reali R, Gessa GL (1998) Reduction of voluntary ethanol intake in ethanol-preferring sP rats by the cannabinoid antagonist SR-141716. Alcohol Alcohol 33:126–130. CrossRef Medline

Cravatt BF, Giang DK, Mayfield SP, Boger DL, Lerner RA, Gilula NB (1996) Molecular characterization of an enzyme that degrades neuromodulatory fatty-acid amides. Nature 384:83–87. CrossRef Medline

De Petrocellis L, Melck D, Palmisano A, Bisogno T, Laezza C, Bifulco M, Di Marzo V (1998) The endogenous cannabinoid anandamide inhibits human breast cancer cell proliferation. Proc Natl Acad Sci U S A 95:8375–8380. CrossRef Medline

Di Marzo V, Fontana A, Cadas H, Schinelli S, Cimino G, Schwartz JC, Piomelli D (1994) Formation and inactivation of endogenous cannabinoid anandamide in central neurons. Nature 372:686–691. CrossRef Medline

Ennaceur A, Delacour J (1988) A new one-trial test for neurobiological studies of memory in rats. 1: Behavioral data. Behav Brain Res 31:47–59. CrossRef Medline

Fernández-Ruiz J, Berrendero F, Hernández ML, Ramos JA (2000) The endogenous cannabinoid system and brain development. Trends Neurosci 23:14–20. CrossRef Medline

Fernández-Ruiz J, Gómez M, Hernández M, de Miguel R, Ramos JA (2004) Cannabinoids and gene expression during brain development. Neurotox Res 6:389–401. CrossRef Medline

Gaffan D, Saunders RC, Gaffan EA, Harrison S, Shields C, Owen MJ (1984) Effects of fornix transection upon associative memory in monkeys: role of the hippocampus in learned action. Q J Exp Psychol B 36:173–221. Medline

Galindo R, Zamudio PA, Valenzuela CF (2005) Alcohol is a potent stimulant of immature neuronal networks: implications for fetal alcohol spectrum disorder. J Neurochem 94:1500–1511. CrossRef Medline

Galve-Roperh I, Sánchez C, Cortés ML, Gómez del Pulgar T, Izquierdo M, Guzmán M (2000) Anti-tumoral action of cannabinoids: involvement of sustained ceramide accumulation and extracellular signal-regulated kinase activation. Nat Med 6:313–319. CrossRef Medline

Gil-Mohapel J, Boehme F, Kainer L, Christie BR (2010) Hippocampal cell loss and neurogenesis after fetal alcohol exposure: insights from different rodent models. Brain Res Rev 64:283–303. CrossRef Medline

Giuffrida A, Parsons LH, Kerr TM, Rodríguez de Fonseca F, Navarro M, Piomelli D (1999) Dopamine activation of endogenous cannabinoid signaling in dorsal striatum. Nat Neurosci 2:358–363. CrossRef Medline

Goodman AM, Delis DC, Mattson SN (1999) Normative data for 4-year-old children on the California Verbal Learning Test-Children's Version. Clin Neuropsychol 13:274–282. CrossRef Medline

Grossmann J (2002) Molecular mechanisms of "detachment-induced apoptosis–Anoikis." Apoptosis 7:247–260. CrossRef

Guo W, Crossey EL, Zhang L, Zucca S, George OL, Valenzuela CF, Zhao X (2011) Alcohol exposure decreases CREB binding protein expression and histone acetylation in the developing cerebellum. PloS One 6:e19351. CrossRef Medline

Hampson RE, Miller F, Palchik G, Deadwyler SA (2011) Cannabinoid receptor activation modifies NMDA receptor mediated release of intracellular calcium: implications for endocannabinoid control of hippocampal neural plasticity. Neuropharmacology 60:944–952. CrossRef Medline

Hansen HH, Krutz B, Sifringer M, Stefovska V, Bittigau P, Pragst F, Marsicano G, Lutz B, Ikonomidou C (2008) Cannabinoids enhance susceptibility of immature brain to ethanol neurotoxicity. Ann Neurol 64:42–52. CrossRef Medline

Harkany T, Keimpema E, Barabás K, Mulder J (2008) Endocannabinoid functions controlling neuronal specification during brain development. Mol Cell Endocrinol 286:S84–S90. CrossRef Medline

Herkenham M, Lynn AB, Little MD, Johnson MR, Melvin LS, de Costa BR, Rice KC (1990) Cannabinoid receptor localization in brain. Proc Natl Acad Sci U S A 87:1932–1936. CrossRef Medline

Howlett AC, Qualy JM, Khachatrian LL (1986) Involvement of Gi in the inhibition of adenylate cyclase by cannabimimetic drugs. Mol Pharmacol 29:307–313. Medline

Huang EJ, Reichardt LF (2001) Neurotrophins: roles in neuronal development and function. Annu Rev Neurosci 24:677–736. CrossRef Medline

Huston JP, Mondadori C, Waser PG (1974) Facilitation of learning by reward post-trial memory processes. Experientia 30:1038–1040. CrossRef

Ikonomidou C, Stefovska V, Turski L (2000a) Neuronal death enhanced by *N*-methyl-D-aspartate antagonists. Proc Natl Acad Sci U S A 97:12885–12890. CrossRef Medline

Ikonomidou C, Bittigau P, Ishimaru MJ, Wozniak DF, Koch C, Genz K, Price MT, Stefovska V, Hörster F, Tenkova T, Dikranian K, Olney JW (2000b) Ethanol-induced apoptotic neurodegeneration and fetal alcohol syndrome. Science 287:1056–1060. CrossRef Medline

Ikonomidou C, Bittigau P, Koch C, Genz K, Hoerster F, Felderhoff-Mueser U, Tenkova T, Dikranian K, Olney JW (2001) Neurotransmitters and apoptosis in the developing brain. Biochem Pharmacol 62:401–405. CrossRef Medline

Izumi Y, Kitabayashi R, Funatsu M, Izumi M, Yuede C, Hartman RE, Wozniak DF, Zorumski CF (2005) A single day of ethanol exposure during development has persistent effects on bi-directional plasticity, *N*-methyl-D-aspartate receptor function and ethanol sensitivity. Neuroscience 136:269–279. CrossRef Medline

Jacob C, Christen CN, Pereira JA, Somandin C, Baggiolini A, Lötscher P,

Ozçelik M, Tricaud N, Meijer D, Yamaguchi T, Matthias P, Suter U (2011) HDAC1 and HDAC2 control the transcriptional program of myelination and the survival of Schwann cells. Nat Neurosci 14:429–436. CrossRef Medline

Jaffard R, Dubois M, Galey D (1981) Memory of a choice direction in a T-maze as measured by spontaneous alternation in mice: effects of intertrial interval and reward. Behav Proc 6:11–21. CrossRef

Ketty SS (1976) Neural mechanisms of learning and memory. In: Biological concomitants of affective states and their possible role in memory processes (Rosenzweig M, Bennett EL, eds), pp 321–326. Cambridge, MA: Massachusetts Institute of Technology.

Kim D, Thayer SA (2001) Cannabinoids inhibit the formation of new synapses between hippocampal neurons in culture. J Neurosci 21:RC146(1–5). Medline

Lallemand F, de Witte P (2005) Ethanol induces higher BEC in CB1 cannabinoid receptor knockout mice while decreasing ethanol preference. Alcohol Alcohol 40:54–62. Medline

Leung D, Saghatelian A, Simon GM, Cravatt BF (2006) Inactivation of N-acyl phosphatidylethanolamine phospholipase D reveals multiple mechanisms for the biosynthesis of endocannabinoids. Biochemistry 45: 4720–4726. CrossRef Medline

Livy DJ, Miller EK, Maier SE, West JR (2003) Fetal alcohol exposure and temporal vulnerability: effects of binge-like alcohol exposure on the developing rat hippocampus. Neurotoxicol Teratol 25:447–458. CrossRef Medline

Lubin FD, Sweatt JD (2007) The IkappaB kinase regulates chromatin structure during reconsolidation of conditioned fear memories. Neuron 55: 942–957. CrossRef Medline

Luikart BW, Zhang W, Wayman GA, Kwon CH, Westbrook GL, Parada LF (2008) Neurotrophin-dependent dendritic filopodial motility: a convergence on PI3K signaling. J Neurosci 28:7006–7012. CrossRef Medline

Lundquist F (1959) The determination of ethyl alcohol in blood and tissue. Methods Biochem Anal 7:217–251. CrossRef

Mameli M, Zamudio PA, Carta M, Valenzuela CF (2005) Developmentally regulated actions of alcohol on hippocampal glutamatergic transmission. J Neurosci 25:8027–8036. CrossRef Medline

Marushige K, Marushige Y (1999) Changes in the mitogen-activated protein kinase and phosphatidylinositol 3-kinase/Akt signaling associated with the induction of apoptosis. Anticancer Res 19:3865–3871. Medline

Mato S, Del Olmo E, Pazos A (2003) Ontogenetic development of cannabinoid receptor expression and signal transduction functionality in the human brain. Eur J Neurosci 17:1747–1754. CrossRef Medline

Mattson SN, Riley EP (1998) A review of the neurobehavioral deficits in children with fetal alcohol syndrome or prenatal exposure to alcohol. Alcohol Clin Exp Res 22:279–294. CrossRef Medline

Mattson SN, Riley EP, Gramling L, Delis DC, Jones KL (1998) Neuropsychological comparison of alcohol-exposed children with or without physical features of fetal alcohol syndrome. Neuropsychology 12:146–153. CrossRef Medline

Mattson SN, Goodman AM, Caine C, Delis DC, Riley EP (1999) Executive functioning in children with heavy prenatal alcohol exposure. Alcohol Clin Exp Res 23:1808–1815. CrossRef Medline

Mattson SN, Crocker N, Nguyen TT (2011) Fetal alcohol spectrum disorders: neuropsychological and behavioral features. Neuropsychol Rev 21: 81–101. CrossRef Medline

May PA, Gossage JP, Kalberg WO, Robinson LK, Buckley D, Manning M, Hoyme HE (2009) Prevalence and epidemiologic characteristics of FASD from various research methods with an emphasis on recent in-school studies. Dev Disabil Res Rev 15:176–192. CrossRef Medline

Mechoulam R, Parker LA (2013) The endocannabinoid system and the brain. Annu Rev Psychol 64:21–47. CrossRef Medline

Medina AE (2011) Fetal alcohol spectrum disorders and abnormal neuronal plasticity. Neuroscientist 17:274–287. CrossRef Medline

Morishita J, Okamoto Y, Tsuboi K, Ueno M, Sakamoto H, Maekawa N, Ueda N (2005) Regional distribution and age-dependent expression of N-acylphosphatidylethanolamine-hydrolyzing phospholipase D in rat brain. J Neurochem 94:753–762. CrossRef Medline

Morozov YM, Freund TF (2003) Postnatal development and migration of cholecystokinin-immunoreactive interneurons in rat hippocampus. Neuroscience 120:923–939. CrossRef Medline

Morozov YM, Ben-Ari Y, Freund TF (2004) The spatial and temporal pattern of fatty acid amide hydrolase expression in rat hippocampus during postnatal development. Eur J Neurosci 20:459–466. CrossRef Medline

Mulder J, Aguado T, Keimpema E, Barabás K, Ballester Rosado CJ, Nguyen L, Monory K, Marsicano G, Di Marzo V, Hurd YL, Guillemot F, Mackie K, Lutz B, Guzmán M, Lu HC, Galve-Roperh I, Harkany T (2008) Endocannabinoid signaling controls pyramidal cell specification and long-range axon patterning. Proc Natl Acad Sci U S A 105:8760–8765. CrossRef Medline

Nyilas R, Dudok B, Urbán GM, Mackie K, Watanabe M, Cravatt BF, Freund TF, Katona I (2008) Enzymatic machinery for endocannabinoid biosynthesis associated with calcium stores in glutamatergic axon terminals. J Neurosci 28:1058–1063. CrossRef Medline

Ohno-Shosaku T, Maejima T, Kano M (2001) Endogenous cannabinoids mediate retrograde signals from depolarized postsynaptic neurons to presynaptic terminal. Neuron 29:729–738. CrossRef Medline

Olney JW, Tenkova T, Dikranian K, Qin YQ, Labruyere J, Ikonomidou C (2002) Ethanol-induced apoptotic neurodegeneration in the developing C57BL/6 mouse brain. Brain Res Dev Brain Res 133:115–126. CrossRef Medline

Pava MJ, Woodward JJ (2012) A review of the interactions between alcohol and the endocannabinoid system: implications for alcohol dependence and future directions for research. Alcohol 46:185–204. CrossRef Medline

Petkov VD, Konstantinova ER, Petkov VV, Vaglenova JV (1991) Learning and memory in rats exposed pre- and postnatally to alcohol. An attempt at pharmacological control. Methods Find Exp Clin Pharmacol 13:43–50. Medline

Piomelli D (2003) The molecular logic of endocannabinoid signalling. Nat Rev Neurosci 4:873–884. CrossRef Medline

Psychoyos D, Vinod KY, Cao J, Xie S, Hyson RL, Wlodarczyk B, He W, Cooper TB, Hungund BL, Finnell RH (2012) Cannabinoid receptor 1 signaling in embryo neurodevelopment. Birth defects research Part B, Developmental and reproductive toxicology 95:137–150. CrossRef Medline

Puighermanal E, Marsicano G, Busquets-Garcia A, Lutz B, Maldonado R, Ozaita A (2009) Cannabinoid modulation of hippocampal long-term memory is mediated by mTOR signaling. Nat Neurosci 12:1152–1158. CrossRef Medline

Puzzo D, Staniszewski A, Deng SX, Privitera L, Leznik E, Liu S, Zhang H, Feng Y, Palmeri A, Landry DW, Arancio O (2009) Phosphodiesterase 5 inhibition improves synaptic function, memory, and amyloid-beta load in an Alzheimer's disease mouse model. J Neurosci 29:8075–8086. CrossRef Medline

Reibaud M, Obinu MC, Ledent C, Parmentier M, Böhme GA, Imperato A (1999) Enhancement of memory in cannabinoid CB1 receptor knockout mice. Eur J Pharmacol 379:R1–R2. CrossRef Medline

Sadrian B, Subbanna S, Wilson DA, Basavarajappa BS, Saito M (2012) Lithium prevents long-term neural and behavioral pathology induced by early alcohol exposure. Neuroscience 206:122–135. CrossRef Medline

Schneider M (2009) Cannabis use in pregnancy and early life and its consequences: animal models. Eur Arch Psychiatry Clin Neurosci 259:383–393. CrossRef Medline

Sik A, van Nieuwehuyzen P, Prickaerts J, Blokland A (2003) Performance of different mouse strains in an object recognition task. Behav Brain Res 147:49–54. CrossRef Medline

Simon GM, Cravatt BF (2010) Characterization of mice lacking candidate N-acyl ethanolamine biosynthetic enzymes provides evidence for multiple pathways that contribute to endocannabinoid production in vivo. Mol Biosyst 6:1411–1418. CrossRef Medline

Starowicz K, Nigam S, Di Marzo V (2007) Biochemistry and pharmacology of endovanilloids. Pharmacol Ther 114:13–33. CrossRef Medline

Stefanis NC, Delespaul P, Henquet C, Bakoula C, Stefanis CN, Van Os J (2004) Early adolescent cannabis exposure and positive and negative dimensions of psychosis. Addiction 99:1333–1341. CrossRef Medline

Subbanna S, Shivakumar M, Umapathy NS, Saito M, Mohan PS, Kumar A, Nixonc RA, Verin AD, Psychoyos D, Basavarajappa BS (2013) G9a-mediated histone methylation regulates ethanol-induced neurodegeneration in the neonatal mouse brain. Neurobiol Dis. Advance online publication. Retrieved March 10, 2013. doi:10.1016/j.nbd.2013.01.022. CrossRef Medline

Tsou K, Brown S, Sañudo-Peña MC, Mackie K, Walker JM (1998) Immunohistochemical distribution of cannabinoid CB1 receptors in the rat central nervous system. Neuroscience 83:393–411. CrossRef Medline

Tsuboi K, Okamoto Y, Ikematsu N, Inoue M, Shimizu Y, Uyama T, Wang J,

Deutsch DG, Burns MP, Ulloa NM, Tokumura A, Ueda N (2011) Enzymatic formation of N-acylethanolamines from N-acylethanolamine plasmalogen through N-acylphosphatidylethanolamine-hydrolyzing phospholipase D-dependent and -independent pathways. Biochim Biophys Acta 1811:565–577. CrossRef Medline

Twitchell W, Brown S, Mackie K (1997) Cannabinoids inhibit N- and P/Q-type calcium channels in cultured rat hippocampal neurons. J Neurophysiol 78:43–50. Medline

Vaglenova J, Pandiella N, Wijayawardhane N, Vaithianathan T, Birru S, Breese C, Suppiramaniam V, Randal C (2008) Aniracetam reversed learning and memory deficits following prenatal ethanol exposure by modulating functions of synaptic AMPA receptors. Neuropsychopharmacology 33:1071–1083. CrossRef Medline

Vinod KY, Arango V, Xie S, Kassir SA, Mann JJ, Cooper TB, Hungund BL (2005) Elevated levels of endocannabinoids and CB1 receptor-mediated G-protein signaling in the prefrontal cortex of alcoholic suicide victims. Biol Psychiatry 57:480–486. CrossRef Medline

Vitalis T, Lainé J, Simon A, Roland A, Leterrier C, Lenkei Z (2008) The type 1 cannabinoid receptor is highly expressed in embryonic cortical projection neurons and negatively regulates neurite growth in vitro. Eur J Neurosci 28:1705–1718. CrossRef Medline

Vitolo OV, Sant'Angelo A, Costanzo V, Battaglia F, Arancio O, Shelanski M (2002) Amyloid beta-peptide inhibition of the PKA/CREB pathway and long-term potentiation: reversibility by drugs that enhance cAMP signaling. Proc Natl Acad Sci U S A 99:13217–13221. CrossRef Medline

Wang L, Liu J, Harvey-White J, Zimmer A, Kunos G (2003) Endocannabinoid signaling via CB1 receptors is involved in ethanol preference and its age-dependent decline in mice. Proc Natl Acad Sci U S A 100:1393–1398. CrossRef Medline

Wang X, Dow-Edwards D, Anderson V, Minkoff H, Hurd YL (2006) Discrete opioid gene expression impairment in the human fetal brain associated with maternal marijuana use. Pharmacogenomics J 6:255–264. CrossRef Medline

Wilson DA, Peterson J, Basavaraj BS, Saito M (2011) Local and regional network function in behaviorally relevant cortical circuits of adult mice following postnatal alcohol exposure. Alcohol Clin Exp Res 35:1974–1984. CrossRef Medline

Wilson RI, Nicoll RA (2001) Endogenous cannabinoids mediate retrograde signalling at hippocampal synapses. Nature 410:588–592. CrossRef Medline

Worster DT, Schmelzle T, Solimini NL, Lightcap ES, Millard B, Mills GB, Brugge JS, Albeck JG (2012) Akt and ERK control the proliferative response of mammary epithelial cells to the growth factors IGF-1 and EGF through the cell cycle inhibitor p57Kip2. Sci Signal 5:ra19. CrossRef Medline

Wu CS, Jew CP, Lu HC (2011) Lasting impacts of prenatal cannabis exposure and the role of endogenous cannabinoids in the developing brain. Future Neurol 6:459–480. CrossRef Medline

Young C, Straiko MM, Johnson SA, Creeley C, Olney JW (2008) Ethanol causes and lithium prevents neuroapoptosis and suppression of pERK in the infant mouse brain. Neurobiol Dis 31:355–360. CrossRef Medline

Zhou FC, Sari Y, Zhang JK, Goodlett CR, Li T (2001) Prenatal alcohol exposure retards the migration and development of serotonin neurons in fetal C57BL mice. Brain Res Dev Brain Res 126:147–155. CrossRef Medline

Zhou FC, Sari Y, Powrozek TA (2005) Fetal alcohol exposure reduces serotonin innervation and compromises development of the forebrain along the serotonergic pathway. Alcohol Clin Exp Res 29:141–149. CrossRef Medline